

Propagation of the Low-Frequency Radio Signal*

J. RALPH JOHLER†, SENIOR MEMBER, IRE

The following paper was solicited for the PROCEEDINGS by the Tutorial Subcommittee of the IRE Wave Propagation Committee, and appears below as a part of a continuing program of presenting review and tutorial papers on subjects of general interest and importance.—*The Editor*

Summary—The propagation of a radio signal and the propagation in the time domain is reviewed for linear amplitude systems. The particular case of the propagation of a ground wave pulse is considered in detail. A stretching in the form or shape of the pulse is noted as a result of the filtering action of the propagation medium. Theoretical transfer characteristics for the media of propagation of LF signals are introduced and methods of computation are considered. The particular case of a signal transmitted between two points on the earth's surface is considered from the viewpoint of propagation in the time domain.

The field of LF waves propagated around the earth is, in large measure, influenced by the reflection and transmission processes at the ionosphere. Such processes are evaluated theoretically with the aid of Maxwell's equations together with an equation which describes the electron motion in the presence of a static magnetic field, a superposed electrodynamic field together with mechanical collisions between electrons and ions, such as the Langevin equation of motion of the electron. The use of full mathematical rigor in the application of these equations is feasible and indeed desirable at LF. Thus, the application of these equations to an electron-ion model plasma with arbitrary orientation of the superposed magnetic induction results in anisotropic transmission and reflection properties. The full rigor can be applied to model plasmas in which the electron density and collision frequency vary with altitude. This leads to the notion of reflection and transmission at a continuously stratified plasma.

Four distinct magneto-ionic propagation components exist in the ionosphere. These can be identified as ordinary and extraordinary, upgoing and downgoing waves. All of these propagation components are coupled to each other as the electron density changes with penetration depth into the plasma.

The anisotropy as a result of the electron gyration (Lorentz force) caused by the superposed static magnetic field of the earth clearly introduces a nonreciprocity in the propagation of the field between transmitter and receiver since the ionosphere reflection coefficient would not in general be the same if transmitter and receiver were interchanged.

The nature of the signal as a result of ionospheric propagation can be determined from the CW field with the aid of the Fourier transform-integral techniques employed on the ground wave in detail.

I. INTRODUCTION

THE ELECTRICAL properties of the ground, the ionosphere, the space between the ground and the ionosphere, and outer space determine the propa-

gation of low-frequency (LF) electromagnetic waves in the vicinity of the earth. The electrical properties of these media (Fig. 1) are by convention described in concise form by means of the angular wave number $k = k_1, k_2, k_3, \dots$, written $k = \eta\omega/c$, which involves the index of refraction $\eta = \eta_1, \eta_2, \eta_3, \dots$, the angular frequency $\omega = 2\pi f$, and the speed of light $c \sim 3(10^8)$ m/sec. A time-harmonic electromagnetic wave, *i.e.*, a wave which oscillates harmonically in time t from $t = -\infty$ to $t = +\infty$ (a wave uninterrupted in time) can be described in terms of the electric field \bar{E} , volts/meter,

$$E = |\bar{E}| \exp(i\omega t - ikD),$$

at a distance D when such a wave is propagated through a particular medium k of infinite extent. The principal task of the theoretician in the development of a description of the propagated field comprises the determination of the wave number or index of refraction from the electrical properties of the medium, applying Maxwell's equations for the propagation of electromagnetic fields \bar{E}, \bar{H} (\bar{H} = electrodynamic magnetic field) to the boundaries between and within the various media and introducing the nature of the source of the radiation.

In the past, attention has been focused upon the propagation of these waves around the surface of the earth taking account of the ground, the ionosphere and the space between the ground and the ionosphere. Recently, as might be expected, considerable interest has developed in the propagation of LF waves in outer space, and there seems to be little doubt that interest in this type of propagation will increase with time.

The theoretical treatment of low frequencies apparently differs quite markedly from the theoretical treatment usually employed at high frequencies as to the degree of mathematical rigor. Indeed, the mathematical rigor required for a theory of propagation of radio waves in the vicinity of the earth increases rapidly as the frequency is decreased. This is not difficult to appreciate intuitively since the wavelength becomes quite long and even approaches in magnitude certain critical dimensions of the medium at LF/VLF, such as the altitude of the lower boundary of the ionosphere

* Received by the IRE, October 23, 1961; revised manuscript received, January 29, 1962. This work was sponsored by the U. S. Air Force as part of Tasks 4 and 5 of the Rome Air Development Center, D.O. AF30-(602)-2488, March, 1961.

† National Bureau of Standards, Boulder, Colo.

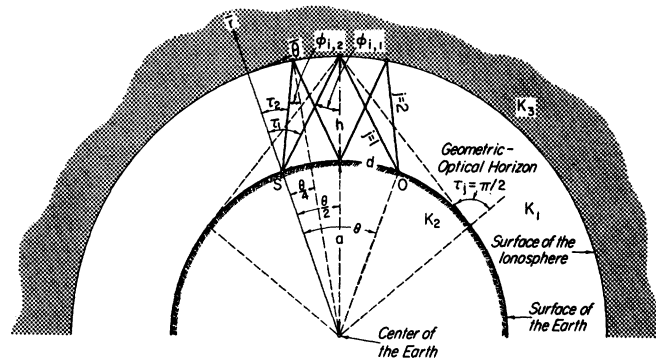


Fig. 1—Propagation media in the vicinity of the earth, illustrating propagation of waves about the earth.

h (Fig. 1). Thus, for example, at 100 kc, $\lambda = f/c \sim 3000$ m at 10 kc, $\lambda \sim 30,000$ m. Therefore, the conventional geometric-optical treatment requires more rigorous corrections since such a treatment in the classical sense implies rays or waves of zero wavelength ($f = \infty$) or practically speaking, waves the length of which is small compared with the critical dimensions of the medium. Indeed, as the frequency under consideration is decreased to the VLF region and the distance between transmitter and receiver d (Fig. 1) is great, it seems to be quite necessary to abandon ray theory altogether and employ the full mathematical rigor to Maxwell's equations together with the appropriate boundary conditions and electrical description of the media. Such an approach is, of course, more difficult and the geometric-optical methods can be derived from this viewpoint [1], [2] as an approximate theory for higher frequencies and/or shorter distances. Whereas the full rigor results in a more satisfying mathematical treatment, the difficulties of maintaining full rigor increase with increasing frequency. Low frequencies are, therefore, on the one hand, in a part of the frequency domain where full rigor is difficult to apply and, on the other hand, complete confidence in the geometric-optical theory does not obtain. LF viewed from this perspective is, therefore, a difficult and challenging field of study for the particular species of investigator interested in the explanation of observed LF phenomena from the more penetrating viewpoint of electromagnetic theory.

Interest in LF waves has persisted from the early days of the radio science. More recently the requirement of precision radio navigation systems, such as the Loran-C pulsed radio navigation system [3], [4] and the requirements for high reliability in communications, especially in the Arctic, has stimulated interest in the favorable properties of these waves. Interest in these waves is also indicated by the extensive measurements of Belrose [5] and the theoretical work of Budden [6] and Barron [7].

This paper reviews the theory of propagation of LF waves with particular emphasis on the propagation of a signal and propagation in the time domain.

II. PROPAGATION OF LF SIGNALS NEAR THE EARTH

Radio waves are employed to transmit information from point to point (Fig. 1), s to o (source to observer) around the earth. This is accomplished in a restricted sense as a form of modulation of the fields of time-continuous waves, $E(\omega, d)$ volts/meter which depend upon frequency, $f = \omega/2\pi$, cycles/second and distance d , meters. This is accomplished in a most general sense by means of an electromagnetic signal or transient electromagnetic field $E(t, d)$ volts/meter, which field depends upon time t and distance d , both reckoned from the transmitter.

The Hertz dipole [8] has been employed with remarkable success by theoreticians to represent a transmitter of such a signal in the LF frequency domain. Such a transmitter implies a point source (either vertical electric or vertical magnetic polarization) of radiation. But such a point source (except for fields very close to the transmitter) is not difficult to approximate experimentally at LF since the wavelengths are quite long relative to the dimensions of practical antennas. It is further implied that more complicated antennas could be synthesized by application of the superposition principle. A corresponding dipole probe has been utilized to define the field at a distance d from the source s (Fig. 1). Such a signal [$E(t, d)$ volts/meter] if it is to convey useful information, communication, or provide a radio navigation fix or time difference or indeed synchronize a system of clocks at different geographic locations to a common frame of reference [3], is varying in time (is modulated) and indeed is typically discontinuous in time. Thus, the signal $E(t, d)$ is an electromagnetic pulse in the quite general sense of the Fourier integral, assuming linear amplitude media of propagation

$$E(t', d) = \frac{1}{2\pi} \int_{-\infty}^{\infty} \exp(i\omega t') E(\omega, d) f_r(\omega) f_s(\omega) d\omega, \quad (1)$$

or using the symbol \mathcal{F}^{-1} for the inverse Fourier transform or Fourier integral

$$E(t', d) = \mathcal{F}^{-1}f(\omega, d) \quad (2)$$

where $f(\omega, d)$ is the complex Fourier transform of a signal. The source transform $f_s(\omega)$ is determined from the time domain $F_s(t)$ by the direct transformation

$$f_s(\omega) = \int_0^{\infty} \exp(-i\omega t) F_s(t) dt \quad (3)$$

or

$$f_s(\omega) = \mathfrak{F}F_s(t) \quad (4)$$

where the source $F_s(t)$ represents a Hertz dipole current moment, $I_0 l$ ampere-meters as a function of universal source time t and the CW field $E(\omega, d)$ represents the complex transfer characteristic of the propagation medium. Since practical systems for the transfer of information affect the signal, it is necessary to introduce the complex transfer characteristic of the system (principally the receiver) $f_r(\omega)$. The local time t' [9] is reckoned locally from the beginning of the first precursor [10], [11] of the pulse, which can arrive at a point o (Fig. 1) no sooner than a signal propagated over the distance d at the speed of light c , but which will in general arrive later. Thus,

$$t' = t - \eta_1 d/c \quad (5)$$

where $\eta_1 \sim 1$ (for air, $\eta_1 \sim 1.000338$ typically at the surface of the earth).

The completely degenerate case of a signal varying harmonically in time from negative to positive infinity ($t = -\infty$ to $t = +\infty$) is a very special situation which can convey theoretically zero information between the point s , the transmitter, and the receiver o (Fig. 1),

$$E(t'd) \sim E(\omega, d), \quad (6)$$

but which is nonetheless frequently employed as an approximation for "narrow bandwidth" communication systems with the inference that such systems are satisfactorily described by the "zero bandwidth" asymptote and where the notion of bandwidth implies a finite spectrum of frequencies $f(\omega, d)$. Indeed, most theoretical calculations of the field \bar{E} evaluate this transform $\bar{E}(\omega, d)$ with the implication that such a function, evaluated over all frequencies of concern in the Fourier integral (1) from negative to positive infinity, together with a specification of the source as a function of time [$f_s(t)$] yield the nature of the propagated signal.

III. PULSES AND PROPAGATION IN THE TIME DOMAIN

The theoretical notion of the signal as a pulse implies important consequences as to the interpretation of propagation in the time domain. This can be more readily explained from the viewpoint of geometric-optics. Indeed, the use of full mathematical wave theory rigor would yield the same general conclusions as those which are reached with the aid of geometric-optics.

A signal transmitted around the earth between two points (Fig. 1) s to o , could arrive at the point o , ac-

cording to the principle of relativity, no sooner than a signal transmitted at the speed of light over some ray length D . This point was established many years ago (1914) by Sommerfeld [10] and Brillouin [11] in a pair of memorable papers which established the consistency of electromagnetic theory with relativity. Whereas the CW concepts of phase velocity and group velocity in the presence of anomalous dispersion gave velocities which varied between positive and negative infinity, the full transient solution demonstrated that a light wave *signal velocity* properly defined was always less than the speed of light and thus consistent with the principle of relativity. Therefore, the shortest "ray" (Fig. 1) has a length $D=d$, the distance along the surface of the earth (since waves in the earth are completely absorbed). The first wave to arrive at the receiver o is then the ground wave $j=0$. Other waves will arrive later as a result of propagation over some distance such as $D=D_j$ where $j=1, 2, 3, \dots$ (Fig. 1) and correspondingly arrive at the receiver at ever later times $t=t_j$. This fact is not obvious to the observer of a CW "signal" [$E(\omega, d)$] since such a signal cannot resolve the individual ordered rays j which arrive at the receiver. Thus, the observer sees only the resultant vector field $E(\omega, d)$ of the sum of a number of individual fields $E_j(\omega, d)$ of each ordered ray j ,

$$E(\omega, d) = \sum_{j=0}^p E_j(\omega, d), \quad j = 0, 1, 2, 3, \dots, \quad (7)$$

in which the zero order field $j=0$ is the ground wave and each higher order field $j=1, 2, 3, \dots$ or $j \neq 0$ corresponds to ionospheric waves or waves reflected by the ionosphere [12],

$$E_j(\omega, d) = i\omega d D_j^{-1} C \exp(i\omega t'_j) G_j' G_j' \alpha_j F_j C_j, \quad (8)$$

where

$$C = I_0 l b^2 / 4\pi \kappa d^3 = 10^{-7}/d, \quad I_0 l = 1, \quad \kappa = 1/c^2 \mu_0, \quad (9)$$

and the local time for the ground wave t'_0 is

$$t'_0 = t - b, \quad (10)$$

$$b = \eta_1 d/c, \quad (11)$$

where $E_0(\omega, d) = |E_0(\omega, d)| \exp[-i(\omega b + \phi_c)]$, considering ϕ_c a phase lag or phase correction [13], and similarly, the local ionospheric wave time or ionospheric wave delay

$$t'_j \quad (j = 1, 2, 3, \dots) \text{ is,}$$

$$t'_j = t - b_j, \quad (12)$$

$$b_j = \eta_1 D_j/c, \quad (j = 1, 2, 3, \dots). \quad (13)$$

The quantity $b_j - b$, a time, is called the relative ionospheric wave delay, Fig. 2 (relative to the ground wave). The physical length of the particular type of ray D_j represented in Fig. 1 (other types of rays are feasible) can be evaluated geometrically for a reflection at an

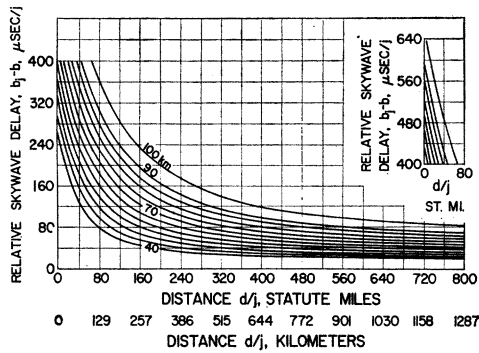


Fig. 2—Relative sky-wave delay for various altitude h of the lower ionosphere boundary.

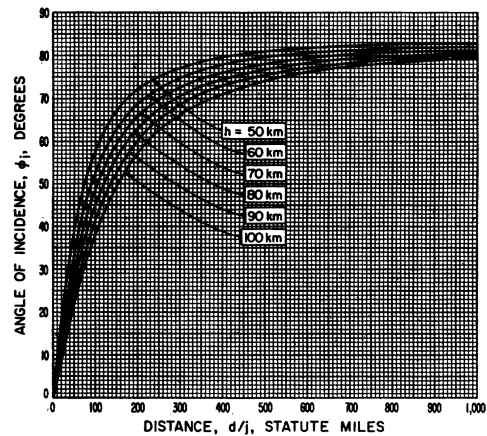


Fig. 3—Geometric-optical relation between the angle of incidence ϕ_i , distance from the source d/j , $j=1, 2, 3, \dots, j \neq 0$, and the altitude h of the lower boundary of the ionosphere.

altitude h above the surface of the earth of radius a ,

$$D_j = 2j[(a + h) \cos \phi_{i,j} - a \cos \tau_j], \quad (14)$$

where (Fig. 1) ϕ_i is the angle of incidence of the ray on the ionosphere and τ_j is the corresponding angle of incidence on the earth and the subscript j reminds the reader that the equation refers to a particular ionospheric wave ($j=1, 2, 3, \dots$) or ground wave ($j=0$) under consideration. The angles ϕ_i and τ_j are evaluated quite simply from the geometry. If,

$$\Delta_j = \left[2a(a + h) \left(1 - \cos \frac{\theta}{2j} \right) + h^2 \right]^{1/2}, \quad \text{then} \quad (15)$$

$$\sin \phi_{i,j} = \Delta_j^{-1} a \sin \frac{\theta}{2j}, \quad (16)$$

$$\cos \phi_{i,j} = \Delta_j^{-1} \left[a \left(1 - \cos \frac{\theta}{2j} \right) + h \right], \quad (17)$$

$$\sin \tau_j = \Delta_j^{-1} (a + h) \sin \frac{\theta}{2j}, \quad (18)$$

$$\cos \tau_j = \Delta_j^{-1} \left[a \left(\cos \frac{\theta}{2j} - 1 \right) + h \cos \frac{\theta}{2j} \right], \quad (19)$$

where θ (Fig. 1) is the angle at the center of the earth subtended by the distance d along the surface of a spherical earth, or simply $d = a\theta$. The relation between distance d/j , angle of incidence ϕ_i , and height h of the lower boundary of the ionosphere can therefore be quite simply illustrated as in Fig. 3.

The transmitting and receiving antenna factors G_j have been included to take account of antennas other than Hertz dipoles, where for the particular case of a vertical magnetic Hertz dipole $G_j=1$ in the equatorial plane of the dipole and $G_j = \sin \tau_j$ for the vertical electrical dipole.

The geometric-optical theory permits the use of plane reflection coefficients or Fresnel type reflection coefficients for rays reflected at the ground (Fig. 1) or the ionosphere. However, the ionosphere is not plane and it is necessary at low frequencies to introduce certain spherical corrections to the geometric-optical theory. The relation between plane and spherical reflections is defined by the convergence-divergence coefficient α_j

which converts the former to the latter or from the viewpoint of the ray theory, takes account of ray focusing by the ionosphere and a corresponding defocusing of rays by the earth. Bremmer [1] has developed formulas for such a correction. A modification of this focusing or convergence correction A_j has been developed by Wait [14] to take account of rays near the geometric-optical horizon $\tau_j \sim \pi/2$ and beyond. The complete expression can be written

$$\alpha_j = \left(1 + h/a \left[\left(2j \sin \frac{\theta}{2j} \right) / \sin \theta \right]^{1/2} \right) \times \left\{ \left[a \left(1 - \cos \frac{\theta}{2j} \right) + h \right] / \left[(a + h) \cos \frac{\theta}{2j} - a \right] \right\}^{1/2} A_j, \quad (20)$$

in which A_j can be evaluated from the cylindrical Hankel function of order $n = \frac{1}{3}$ of the second kind, which for $j=1$ can be written

$$A_j \sim \left(\frac{\pi}{2} Z_j \right)^{1/2} H_{1/3}^{(2)}(Z_j) \exp \{ -i[5\pi/12 - Z_j] \} \quad (21)$$

where

$$Z_j = k_1 a \cos^3 \tau_j / 3 \sin^2 \tau_j. \quad (22)$$

Wait [14] has developed numerous graphs of the function α_j and A_j and Johler [12] has detailed some computation methods, especially for the Hankel function $H_{1/3}^{(2)}(z)$.

The factor F_j is an antenna pattern factor since it describes a plane wave incident on a sphere with a receiver dipole antenna located on the surface of the sphere. The factor F_j accounts for the presence of the spherical earth at both the transmitter F_j^t and the receiver F_j^r , and if it can be assumed that the geometric-optical ray is not too close or beyond the geometric-optical horizon (Fig. 1), the Fresnel approximation again suffices to determine F_j , or for vertical polarization

$$F_j \sim [1 + R_e^t(\tau_j)][1 + R_e^r(\tau_j)] \quad (23)$$

where the superscripts t and r refer to the transmitter and receiver respectively, and the subscript e refers to vertical electric polarization and

$$R_e(\tau_j) = \left\{ \frac{k_2^2 \cos \tau_j / k_1^2 - [k_2^2 / k_1^2 - \sin^2 \tau_j]^{1/2}}{k_2^2 \cos \tau_j / k_1^2 + [k_2^2 / k_1^2 - \sin^2 \tau_j]^{1/2}} \right\}, \quad (24)$$

or for horizontal polarization

$$R_m(\tau_j) = \left\{ \frac{\cos \tau_j - [k_2^2 / k_1^2 - \sin^2 \tau_j]^{1/2}}{\cos \tau_j + [k_2^2 / k_1^2 - \sin^2 \tau_j]^{1/2}} \right\} \quad (25)$$

where

$$k_2 = \frac{\omega}{c} \left[\epsilon_2 - i \frac{\sigma \mu_0 c^2}{\omega} \right]^{1/2}, \quad k_1 = \frac{\omega}{c} \eta_1 \sim \frac{\omega}{c}, \quad (26)$$

which defines the wave number of the air and the ground in terms of the dielectric constant ϵ_2 relative to a vacuum, the conductivity, σ , mhos/m and the permeability $\mu_0 = 4\pi(10^{-7})$ h/m. The dielectric constant is $\epsilon_2 = 15$ for typical land and $\epsilon_2 = 80$ for sea water; also $\sigma = 0.005$ and 5 mhos/m for land and sea water respectively. Here again it has been found necessary to correct the rays near and beyond the geometric-optical horizon $\tau_j \sim \pi/2$. A contour integral developed by Wait [15] can be employed close to the geometric-optical horizon for the calculation of $F_j = F_j^t F_j^r$:

$$F_j^{t,r} \sim (\pi)^{-1/2} \exp[-ik_1 a \theta'] \int_{-\infty \exp[-i2\pi/3]}^{\infty} \frac{\exp[-i(k_1 a/2)^{1/3} \theta' \rho]}{W_1'(\rho) - q W_1(\rho)} d\rho, \quad (27)$$

where $\theta'(d-d_H)/a$, where d_H is the distance from transmitter to geometric-optical horizon ($\tau_j \sim \pi/2$) and

$$q = -i \frac{(k_1 a)^{1/3}}{2} \frac{k_1}{k_2} \sqrt{1 - \frac{k_1^2}{k_2^2}}. \quad (28)$$

$W_1(z)$ and $W_1'(z)$ are airy integrals related to the cylindrical Hankel Functions [12] (also see Appendix).

$$W_1(\rho) = \exp[-2\pi i/3] \sqrt{\pi/3} (-\rho)^{1/2} H_{1/3}^{(2)} \left[\frac{2}{3} (-\rho)^{3/2} \right], \quad (29)$$

$$W_1'(\rho) = \exp[-4\pi i/3] \sqrt{\pi/3} \rho H_{2/3}^{(2)} \left[\frac{2}{3} (-\rho)^{3/2} \right], \quad (30)$$

where

$$-\frac{\pi}{3} \leq \arg \rho < \frac{5\pi}{3},$$

and

$$\arg(-\rho) = \arg \rho - \pi,$$

$$\arg \rho^{m/n} = \frac{m}{n} \arg \rho \quad \text{where } m \text{ and } n \text{ are integers.}$$

These restrictions on $\arg \rho$ make all functions involved single valued. Note that a separate conductivity σ and dielectric constant ϵ_2 can be ascribed to transmitter and

receiver. Wait [15] has developed curves of this function and some computation methods have been outlined by Johler [12]. Close to, but beyond the geometric-optical horizon, the factor $F_j = F_j^t F_j^r$ can be evaluated as noted by Wait [15]. A residue series summation [12]

$$F_j^{t,r} \sim -2i\sqrt{\pi} \exp[-ik_1(d-d_H)] \sum_{s=0}^{\infty} \frac{\exp[-i(k_1 a)^{1/3} \theta' \tau_s]}{(2^{1/3} \tau_s - q^2) W_1(2^{1/3} \tau_s)} \quad (31)$$

where the permittivity lapse factor α , which takes account of the variation in index of refraction of the atmosphere with altitude is $\alpha \sim 0.75$ to 0.85 . Howe [17], Johler, Walters, and Lilley [16], and Walters and Johler [18] have developed methods for taking the special roots $\tau = \tau_s$ of (32), where the limiting roots $\delta = 0$, $\delta = \infty$ are found from

$$\frac{d\delta}{d\tau} - 2\delta^2 \tau + 1 = 0, \quad (32)$$

where the factor δ (which depends on dielectric constant ϵ_2 and conductivity σ) for vertical electric polarization of the Hertz dipole $\delta = \delta_e$,

$$\delta_e = \frac{-ik_2^2 \alpha^{1/3} / k_1^2}{(k_1 a)^{1/3} \left[\frac{k_2^2}{k_1^2} - 1 \right]^{1/2}} \quad (33)$$

where the permittivity lapse factor α , which takes account of the variation in index of refraction of the atmosphere with altitude is $\alpha \sim 0.75$ to 0.85 . Howe [17], Johler, Walters, and Lilley [16], and Walters and Johler [18] have developed methods for taking the special roots $\tau = \tau_s$ of (32), where the limiting roots $\delta = 0$, $\delta = \infty$ are found from

$$H_{2/3}^{(2)} \left[\frac{1}{3} (-2\tau_s)^{3/2} \right] = 0, \quad \delta_e = \infty, \quad (34)$$

$$H_{1/3}^{(2)} \left[\frac{1}{3} (-2\tau_s)^{3/2} \right] = 0, \quad \delta_e = 0, \quad (35)$$

$$s = 0, 1, 2, 3 \dots$$

The reflection process at the ground and the ionosphere is represented (8) in concise form C_j , according to Bremmer [1], for the case of a vertically polarized transmitter and receiver (Fig. 4).

$$C_j = \frac{1}{j! R_e} \frac{d^j}{dx^j} \left[\frac{1 + A_1 x}{1 - A_2 x - A_3 x^2} \right]_{x=0}, \quad (36)$$

where

$$A_1 = -R_m T_{mm}$$

$$A_2 = R_e T_{ee} + R_m T_{mm}$$

$$A_3 = R_e R_m [-T_{ee} T_{mm} + T_{em} T_{mv}]$$

where R_e and R_m are the conventional Fresnel ground reflection coefficients for plane waves of angle of incidence τ_j (Fig. 1) of both vertical and horizontal polarization respectively, and the T 's represent, the ionosphere reflection coefficients for plane waves with angle of incidence ϕ_s ; thus, the essential nature of the propagation of the CW signal around the earth via the ionosphere can be described in terms of four reflection coefficients T_{ee} , T_{em} , T_{me} , T_{mm} . The reflection coefficient T_{ee} refers to vertical electric polarization of the incident

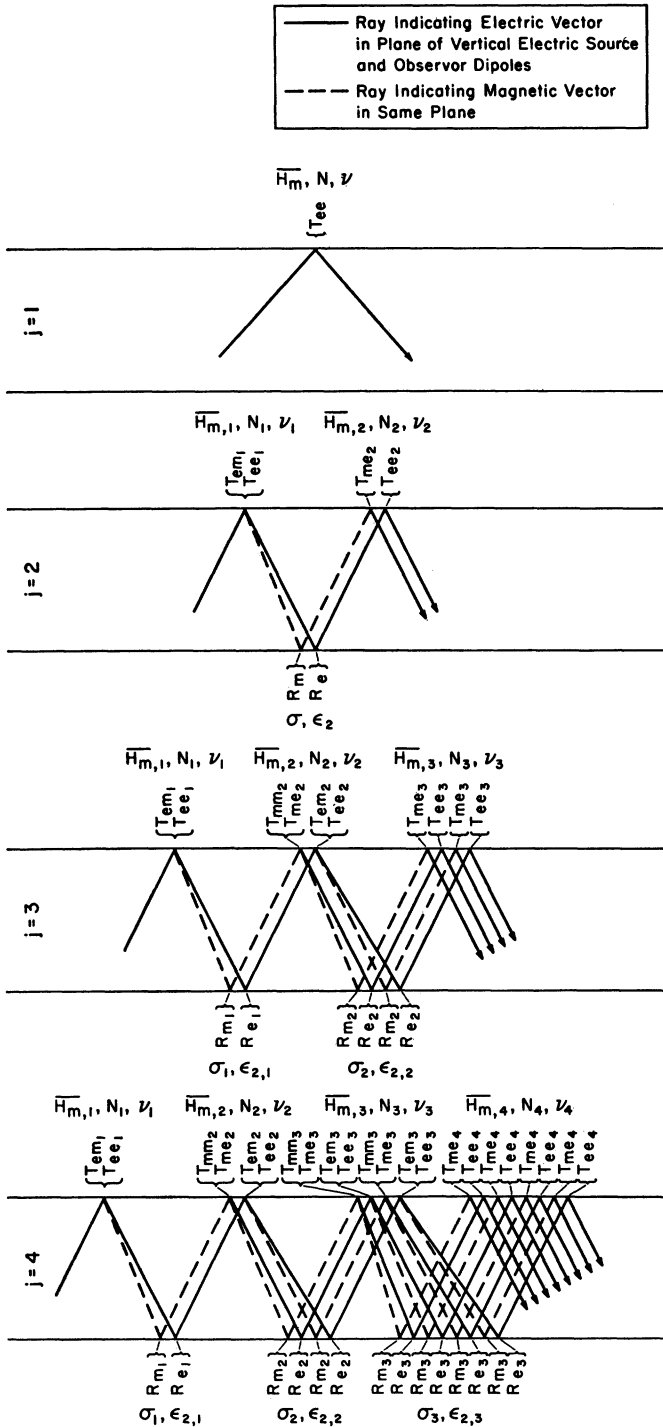


Fig. 4—Geometric-optical ray propagation mechanism, illustrating the development of the factor C_j and illustrating coupling exterior to the ionosphere as a consequence of the generation of the abnormal components.

plane wave and a similar vertical electric polarization of the reflected wave. The coefficient T_{em} describes the generation of the abnormal component by the incident vertical polarization (reflected horizontal electric polarization for vertical electric excitation). Similarly, T_{mm} refers to the incident horizontal electric polarization and the corresponding reflected horizontal electric polarization. Also, the abnormal component of the horizontal electric polarization (reflected vertical electric polarization for horizontal electric excitation) is described by the coefficient T_{me} . Referring these matters to a local coordinate system (Fig. 5) at the ionosphere lower boundary [12], [19], [20],

$$\begin{aligned}
 T_{ee} &= E_{y'r}/E_{y'i}, & T_{mm} &= E_{x'r}/E_{x'i}, \\
 T_{em} &= E_{x'r}/E_{y'i}, & T_{me} &= E_{y'r}/E_{x'i},
 \end{aligned}
 \tag{37}$$

where the subscripts i or r refer to the incident and reflected wave, respectively, at the lower boundary of the ionosphere. The techniques for evaluating the reflection coefficients for an anisotropic model electron-ion plasma are quite complicated and will be discussed later.

The ground wave CW, $E_o(\omega, d)$ (i.e., the zero order ray $j=0$ can be evaluated from the classical series of residues) formulated by Bremmer can be written in the form [1], [13], [23] for vertical electric polarization

$$\begin{aligned}
 E(\omega, d) &= 2i\omega C \left[2\pi\alpha^{2/3}(k_1a)^{1/3} \frac{d}{a} \right]^{1/2} \\
 &\times \sum_{s=0}^{\infty} \frac{\exp \left\{ -i \left[(k_1a)^{1/3} \tau_s \alpha^{2/3} \frac{d}{a} + \frac{\alpha d}{2a} + \frac{\pi}{4} \right] \right\}}{[2\tau_s - 1/\delta_e]},
 \end{aligned}
 \tag{38}$$

where $s=0, 1, 2, 3, \dots$, C is given by (9), and again $\alpha \sim 0.75$ to 0.85 and δ_e, τ_s have been defined (32), (33).

A horizontally-polarized Hertz dipole radiation field can also be found (vertical magnetic field, H_r , ampere-turns/meters) simply by replacing δ_e by δ_m . $\delta_m = \delta_e k_i^2/k_e^2$, re-evaluating τ_s and substituting in (38).

The notion of a CW signal $E(\omega, d)$ as the vector sum of individual rays ordered in time (7) is obscure to the observer of such a signal. However, a signal in the true sense, i.e., one which can convey information and hence is interrupted in the time domain, manifests the individual propagation rays. The Fourier integral (1) for a pulse transmission can be rewritten as a consequence of propagation of such signals $E(t, d)$,

$$\begin{aligned}
 E(t', d) &= \sum_{j=0}^p E_j(t'_j, d) \\
 &= \sum_{j=0}^p \frac{1}{2\pi} \int_{-\infty}^{\infty} \exp(i\omega t'_j) E_j(\omega, d) f_r(\omega) f_s(\omega) d\omega.
 \end{aligned}
 \tag{39}$$

This merely represents the sum of separate Fourier integrals for each ray, separated in time by the ionospheric wave delay t'_j .

The signal $E(t', d)$, (1), (39) which has been described in the time domain, is in general complex if complex source functions $F_s(t)$, (3) are employed. The signal

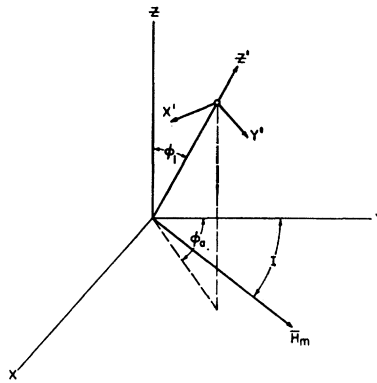


Fig. 5—Local coordinate system for ionosphere boundary.

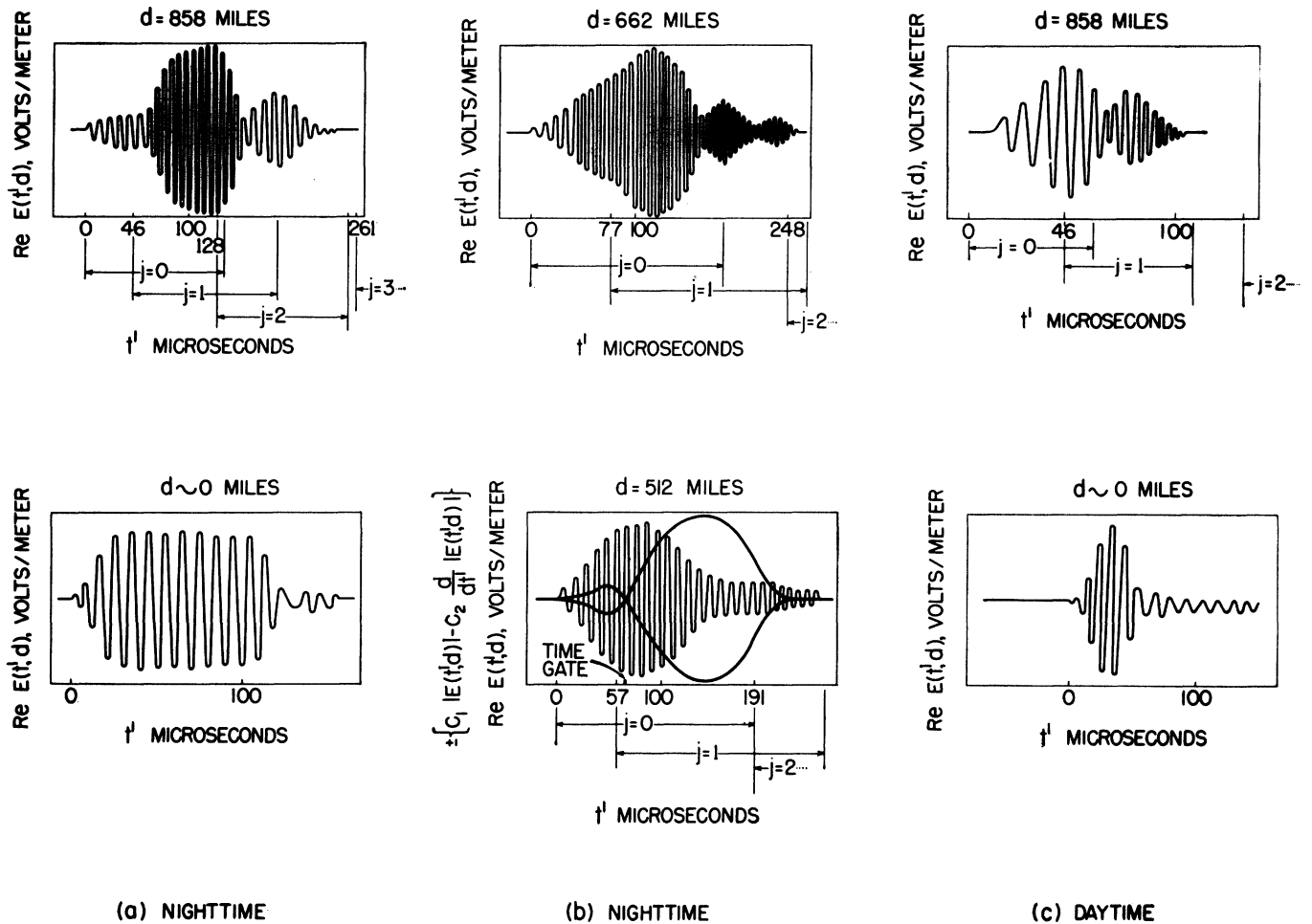


Fig. 6—Observations of propagated pulses of various lengths illustrating the time separation of the ground wave ($j=0$) and the various ionospheric reflections ($j=1, 2, 3, \dots$). The measurement of a point in time on the leading edge of the pulse with the amplitude envelope minus the derivative of the amplitude envelope method is also illustrated ($b, d=512$). (Oscillograms traced from original photographs of July–August, 1953, CYTAC/Loran-C field tests).

which is observed and recorded as an oscillogram, for example, is typically the real part of the complex field, $\text{Re } E(t', d)$, while the amplitude $|E(t', d)|$, can represent some sort of envelope detection process in the receiver. Thus, an envelope can be synthesized with the aid of a complex source and propagated with the signal as an index of the pulse dispersion (change in form or shape) as a result of the propagation.

The physical notion of a signal observed at a point o (Fig. 1) as the sum of ordered rays in the time domain is illustrated [21] in Fig. 6 for various length pulses employed during the development of the Cytac/Loran-C system [22]. The pulse radiated at the source, undisturbed by the ionospheric time rays (pure ground wave) is shown as oscillograms $[\text{Re } E(t', d)]$ at short distances. The action of the propagation medium on the signal is demonstrated by the complicated, multiple ($j=0, 1, 2, 3, \dots$), overlapping pulses observed at great distances. Thus, the oscillogram or amplitude-time function $\text{Re } E(t', d)$ observed at a great distance comprises the overlapping individual signals $E_j(t', d)$, $j=0, 1, 2, 3, \dots$, apparently added together according to the complex field specification E_j of each and separated in time by the ionospheric wave delay t'_j of each ray j ordered in the time domain $j=0, 1, 2, 3, \dots$. The approximate area in the amplitude-time plane occupied by each ordered ray is shown in Fig. 6. Areas of overlap in which both constructive and destructive interference between cycles of the multiple pulses produce notches. Enhancements in the composite pulse can be observed.

Notwithstanding the areas of overlap, the instrumentation has been developed which can sort out the individual ordered rays $E_j(\omega, d)$, $j=0, 1, 2, 3, \dots$, in the time domain and study or measure the amplitude, phase and dispersion of these individually [3], [4], [22]. Thus cycles and minute fractions of a cycle can be measured by tagging a point in time on the pulse. One such method utilizes the amplitude envelope and hence employs amplitude envelope detection. In effect, the method forms the difference between the amplitude envelope $|E(t', d)|$ and the derivative $d|E(t', d)|/dt'$, and an elaborate null seeking device [4] seeks out a null point or zero crossing for the time function so desired, thus determining a time-root T_c of the differential equation

$$F(t', d) = c_1 |E(t', d)| - c_2 \frac{d}{dt'} |E(t', d)| = 0, \quad (40)$$

where c_1 and c_2 are constants which move the point in time which is to be tagged on the pulse, such as the time gate shown on Fig. 6(b), which can be set by the operator to pick out a particular point on the pulse. Both amplitude and time (phase) can be measured at such a point. Additional techniques are used to detect cycles and minute fractions of a cycle under the envelope on the leading edge (pure ground wave signal) or elsewhere

on the pulse (a particular ionospheric ray signal can be selected). The existence of an ordered ($j=0, 1, 2, 3, \dots$) sequence of signals $E_j(\omega, d)$ as a result of propagation over such rays as D_j (Fig. 1) has therefore been established both theoretically and experimentally.

IV. THE GROUND WAVE SIGNAL

The particular case of a ground wave pulse, $E(t', d) = E_0(t', d)$, $j=0$ has considerable theoretical and practical interest. The source dipole current $F_s(t)$ can be specified in a variety of forms. The complex damped cosine form has considerable theoretical interest [23].

$$\begin{aligned} \text{Re } F_s(t) &= \text{Re exp } (-\nu t) \\ &= \exp(-c_1 t) \cos \omega_c t, \quad (0 < t < \infty) \\ &= 0, \quad (t < 0) \end{aligned} \quad (41)$$

or for the sine source,

$$\begin{aligned} -\text{Im } F_s(t) &= \text{Re } i \exp(-\nu t) = \exp(-c_1 t) \\ &\cdot \sin = 0, (t < 0) \omega_c t, (0 < t < \infty) \end{aligned} \quad (42)$$

where

$$\nu = c_1 + i\omega_c. \quad (43)$$

The direct transformation can be accomplished for this particular source by evaluating the integrals (3), (4) and inserting in the integrand of the Fourier integral (1),

$$\begin{aligned} E(t', d) &= \frac{1}{2\pi} \int_{-\infty}^{\infty} \exp(i\omega t') E(\omega, d) \\ &\cdot \int_0^{\infty} F_s(t) \exp(-i\omega t) dt d\omega \end{aligned} \quad (44)$$

or upon evaluating the inner integral for the specified source $F_s(t)$, (41)-(43),

$$\begin{aligned} E(t', d) &= \frac{1}{2\pi} \int_0^{\infty} |E(\omega, d)| \\ &\cdot \left\{ \left[\frac{\cos \left[\omega_c t' - \phi_c' + \tan^{-1} \frac{-(\omega_c + \omega)}{c_1} \right]}{\sqrt{c_1^2 + (\omega_c + \omega)^2}} \right] \right. \\ &+ \left. \frac{\cos \left[-\omega t' + \phi_c' + \tan^{-1} \frac{-(\omega_c - \omega)}{c_1} \right]}{\sqrt{c_1^2 + (\omega_c - \omega)^2}} \right] \\ &+ i \left[\frac{\sin \left[\omega t' - \phi_c' + \tan^{-1} \frac{-(\omega_c + \omega)}{c_1} \right]}{\sqrt{c_1^2 + (\omega_c + \omega)^2}} \right] \\ &+ \left. \frac{\sin \left[-\omega t' + \phi_c' + \tan^{-1} \frac{-(\omega_c - \omega)}{c_1} \right]}{\sqrt{c_1^2 + (\omega_c - \omega)^2}} \right] \Bigg\} d\omega, \end{aligned} \quad (45)$$

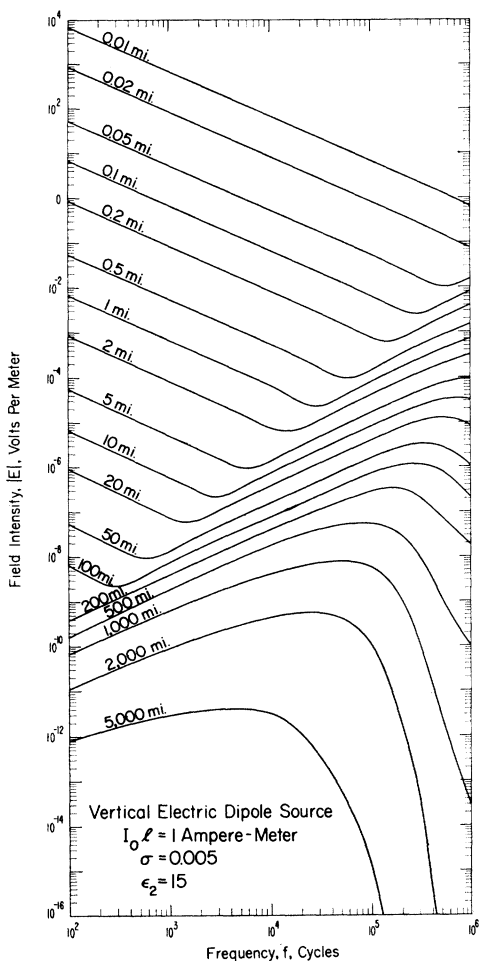


Fig. 7—Amplitude transfer characteristic of the ground wave.

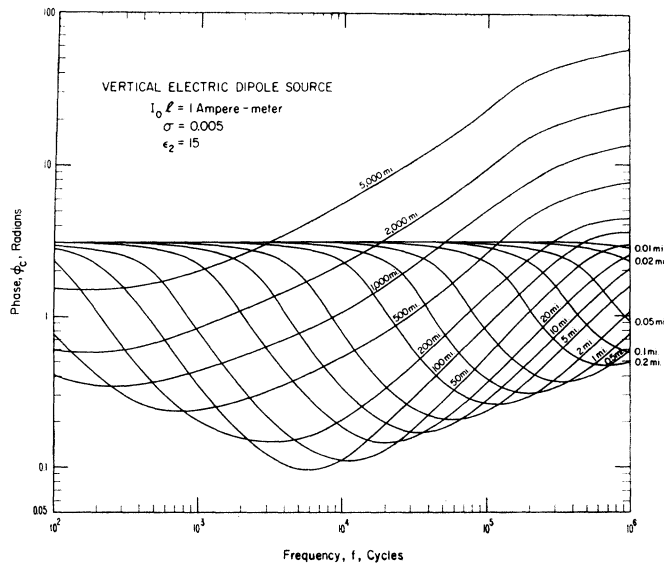


Fig. 8—Phase transfer characteristic of the ground wave.

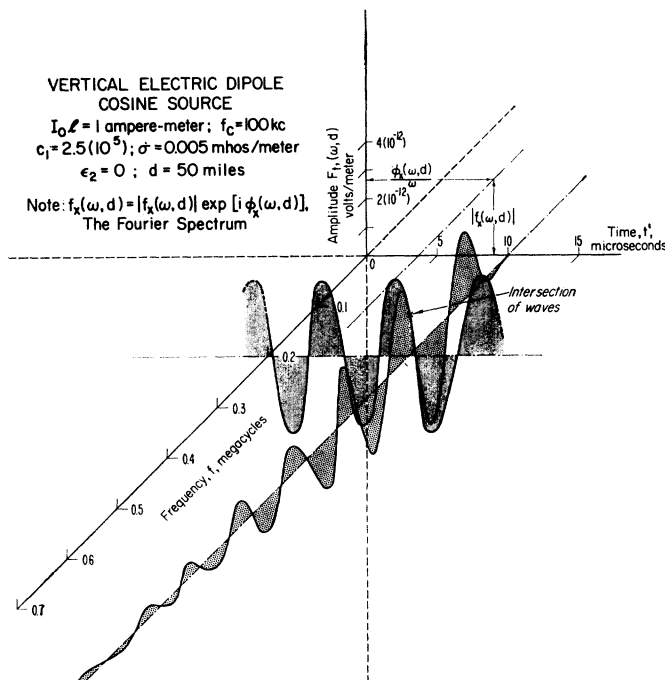


Fig. 9—Integrand of Fourier integral or image of pulse in the frequency-amplitude plane at small distance from the source, illustrating the relation of the integrand to the Fourier spectrum waves.

where $\phi_c' = -\phi_c - \pi/2 = \arg [E(\omega, d)]$ and $E(\omega, d) = E_0(\omega, d)$.

The real part of the amplitude-time function (45) $\text{Re } E(t', d)$ is the desired function for the cosine source (41), and the imaginary part $-\text{Im } E(t', d) = \text{Re } [iE(t', d)]$ is the desired function for the sine source (42). This integral can be evaluated with the aid of quadrature techniques [23]. Thus, the problem has been reduced to the evaluation of a real integral

$$\begin{aligned} E(t', d) &= \int_0^\infty F_t(\omega, d) d\omega \\ &= \text{Re} \int_{-\infty}^\infty f(\omega, d) \exp(i\omega t) d\omega. \end{aligned} \quad (46)$$

The transfer function for the ground wave, $E(\omega, d)$, (38) which can now be inserted directly in the integrand of the Fourier integral is illustrated in Figs. 7 and 8. Since the transfer characteristic $E(\omega, d) = E_0(\omega, d)$ is complex, both amplitude and phase are presented as a function of frequency for various distances. The phase is presented as the phase lag ϕ_c where the total true phase $\arg [E(\omega, d)] = -[k_1 d + \phi_c + \pi/2]$. The effect of the conduction currents in the earth on the propagation has been introduced as the conductivity for typical land, $\sigma = 0.005$ mho/m. The effect of the displacement currents in the earth on the propagation has been introduced by the dielectric constant $\epsilon_2 = 15$ (relative to a vacuum). The permeability $\mu_0 = 4\pi(10^{-7})$ henry/meter has been assumed. The use of the series of residues applicable to propagation about a spherical earth takes account of the vertical lapse of the index of refraction of the earth's atmosphere [1] by the factor α (38) where $\alpha \sim 0.75$. Although it has been assumed that both transmitter and receiver are located on the surface of the earth, the effect of elevating transmitter and/or receiver can be introduced by multiplying *each* term of the series of residues (38) by the factor $f_s(h_1)f_s(h_2)$ where h_1 and h_2 are the height of the transmitter and receiver, respectively, above the surface of the earth, and (1), (13), (18)

$$f_s(h) = \frac{h_2 \left\{ \left(\frac{1}{2} \right)^{2/3} \left[(k_1 a)^{2/3} \frac{2h\alpha^{1/3}}{a} - 2\tau_s \right] \right\}}{h_2 \left\{ -(2)^{1/3} \tau_s \right\}}, \quad (47)$$

in which $h(z)$ is the modified Hankel function tabulated by Furry [24].

The integrand of the Fourier integral (Fig. 9) in the frequency-amplitude plane at some given local time t' can be related to the more conventional notion of the Fourier spectrum $f_x(\omega, d)$ by eliminating the notion of a negative frequency ω . Thus, the amplitude spectrum is

$$|f_x(\omega, d)| = |f(\omega, d) + f(-\omega, d)| \quad (\omega \geq 0) \quad (48)$$

and the phase spectrum is

$$\begin{aligned} \phi_x(\omega, d) &= \arg [f_x(\omega, d)] \\ &= \arg [f(\omega, d) + f(-\omega, d)] \quad (\omega \geq 0). \end{aligned} \quad (49)$$

The phase, $\phi_x(\omega, d)$ can be reckoned (Fig. 9) from the origin $t' = 0$ to the crest of the continuous wave or Fourier spectrum wave at a certain frequency (0.2 Mc, Fig. 9). The corresponding amplitude $|f_x(\omega, d)|$ does not correspond to the amplitude of the integrand $F_t(\omega, d)$. The two waves do intersect, however, at the point $t' = 10 \mu\text{sec}$, (see, *e.g.*, Fig. 9), at which point the Fourier spectrum wave enters the integration (45) with a phase shift beyond the crest of the wave. Thus, the Fourier spectrum waves will all be phase advanced by different amounts between the zero and infinite frequency limits of integration. The Fourier spectrum wave, $f_x(\omega, d)$, could, therefore, represent exactly the signal observed through a receiver, if and only if the receiver transfer function, $f_r(\omega)$, as shown in (1), (39), introduced an "infinite Q " or zero bandwidth circuit into the transform, $F_t(\omega, d)$, such that only a single frequency was admitted. But this is another way of saying the receiver circuit rings or oscillates indefinitely as a result of the "high Q " of the circuit. Thus, in general, it is necessary to perform the integration (1), (39) for each time t' from zero to infinite frequency to describe the signal $E(t', d)$. Fortunately the wave (Fig. 9) $F_t(\omega, d)$ damps out rapidly as the frequency f is increased. Indeed, the particular wave illustrated (Fig. 9) applies to short distances ($d = 50$ statute miles) whereas for greater distances [23] the integrand for the case of the ground wave pulse is rather severely mutilated by the transfer function (Figs. 7, 8) such that the wave $F_t(\omega, d)$ damps out in a cycle or fraction thereof, which is another way of saying the integral $E(t', d)$, (1) converges rapidly. This convergence phenomenon, together with any further mutilation introduced by the receiver transfer characteristic $f_r(\omega)$, can be exploited in the application of quadrature techniques on the integral [23].

The detailed structure of the transient for various combinations of characteristic frequency $f_c = \omega_c/2\pi$ and damping c_1 for both sine and cosine source functions are illustrated in Figs. 10–13 (pp. 414–415). The dispersion of the pulse at great distance is evident in the illustrations. The most noteworthy attribute of this dispersion was an increase in the natural period of the pulse or a stretching of the pulse in the time domain. The propagation medium thus illustrated, assuming a perfect (infinite bandwidth) receiver $f_r(\omega) = 1$ filters the signal, and indeed at the greater distances the exact form of the source becomes obscured by the filtering action.

The cosine source (Figs. 11 and 13) employs an abrupt initial current. The radiated field therefore propagated an impulse type of function which is superposed upon the sinusoid. This can be explained quite simply for the case of an infinitely conducting earth with the

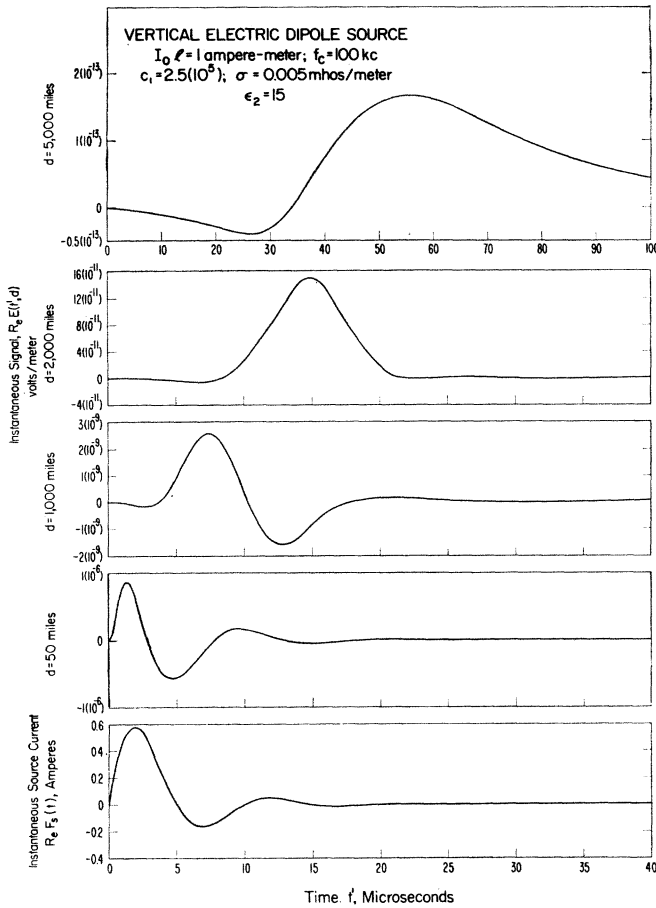


Fig. 10—Instantaneous signal and corresponding damped LF sine wave source current of a propagated ground wave pulse.

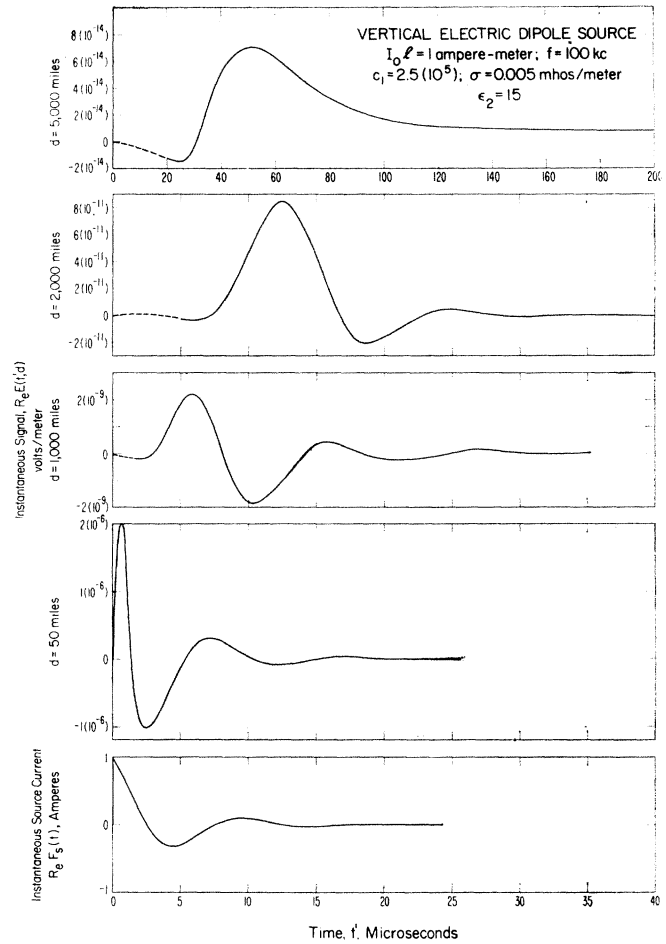


Fig. 11—Instantaneous signal and corresponding damped LF cosine wave source current of a propagated ground wave pulse.

aid of the convenient Laplace transform

$$E(s) = 1 \quad (\nu = 0) \tag{50}$$

where $s = i\omega$. The inverse Laplace transform \mathcal{L}^{-1} is

$$E(t', d) = \mathcal{L}^{-1}E(s) = \delta(t') \tag{51}$$

where the Dirac impulse function $\delta(t')$ can be defined in relation to the step function $u(t)$; thus,

$$\int_0^t \delta(t) dt = u(t), \tag{52}$$

where

$$\begin{aligned} u(t) &= 1, & t > 0 \\ u(t) &= 0, & t < 0. \end{aligned} \tag{53}$$

The impulse is, of course, finite in the damped cosine wave (amplitude and duration finite) as a result of the finite conductivity of the ground, the displacement currents in the ground and the effect of the earth's curvature. The transient response of the ground wave at great distances illustrates (Figs. 12–14, pp. 415–416) the stretching of such pulses in the time domain.

The finite bandwidth of a radio receiver or filter, $f_r(\omega) \neq 1$, can be introduced by a mutilation of the Fourier transform with one or more frequency selective networks. Perhaps the simplest network is the following series network:

$$f_r(\omega) = \frac{\frac{R}{L}(i\omega)}{-\omega^2 + \frac{R}{L}(i\omega) + \frac{1}{CL}}, \tag{54}$$

where R is a resistive element (ohms) L is an inductive element (henry) and C is a capacitive element (farads). The modification of the pulse by the finite bandwidth so described (54) for particular values of R , L and C is illustrated in Figs. 15 and 16, p. 416). The ringing of the circuit becomes evident (Fig. 16) as the constants R , L and C are changed so that the bandwidth becomes quite narrow, *i.e.*, the Fourier spectrum wave, $f_x(\omega, d)$ is approached asymptotically.

The damped sine-squared pulse, of which the envelope shape, defined by $\sin^2 \omega_p$, can serve as a useful model for the type pulse employed in radio navigation systems. Such a pulse can be synthesized quite simply by redefining the source function $F_s(t)$, (41), (42),

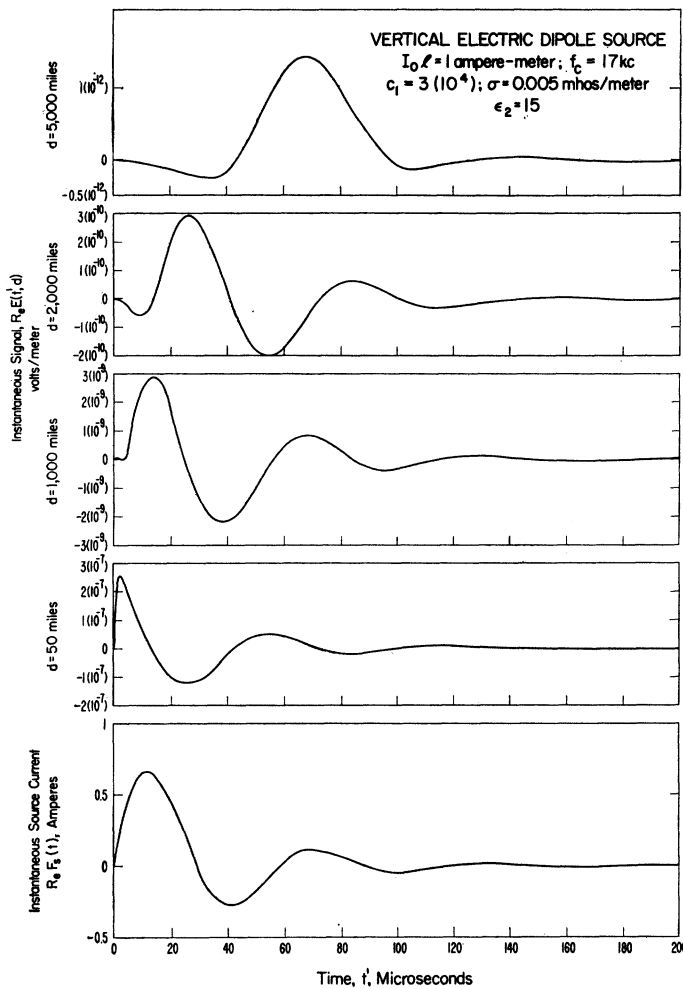


Fig. 12—Instantaneous signal and corresponding damped VLF sine wave source current of a propagated ground wave pulse.

$$\text{Re } F_s(t) = \exp(-c_1 t) \sin^2 \omega_p t \sin \omega_c t \quad (55)$$

$$\begin{aligned} \text{Re } F_s(t) = & \frac{1}{2} \exp(-c_1 t) \sin \omega_c t \\ & - \frac{1}{4} \exp(-c_1 t) \sin(\omega_c + 2\omega_p)t \\ & - \frac{1}{4} \exp(-c_1 t) \sin(\omega_c - 2\omega_p)t. \end{aligned} \quad (56)$$

$$\begin{aligned} F_s(t) = & \frac{i}{2} \exp(-\nu t) - \frac{i}{4} \exp(\nu_1 t) \\ & - \frac{i}{4} \exp(-\nu_2 t), \end{aligned} \quad (57)$$

where

$$\begin{aligned} \nu &= c_1 + i\omega_c \text{ (as before)} \\ \nu_1 &= c_1 + i(\omega_c + 2\omega_p) \\ \nu_2 &= c_1 + i(\omega_c - 2\omega_p). \end{aligned}$$

The typical radio navigation type pulse has a value for c_1 of the order of ω_p . It is quite obvious, however, that the amplitude time function $E(t', d)$ for the damped sine-squared pulse is merely the sum of three waves calculated as previously described (45).

$$E(t', d) = A_1 E_\nu(t', d) + A_2 E_{\nu_1}(t', d) + A_3 E_{\nu_2}(t', d), \quad (58)$$

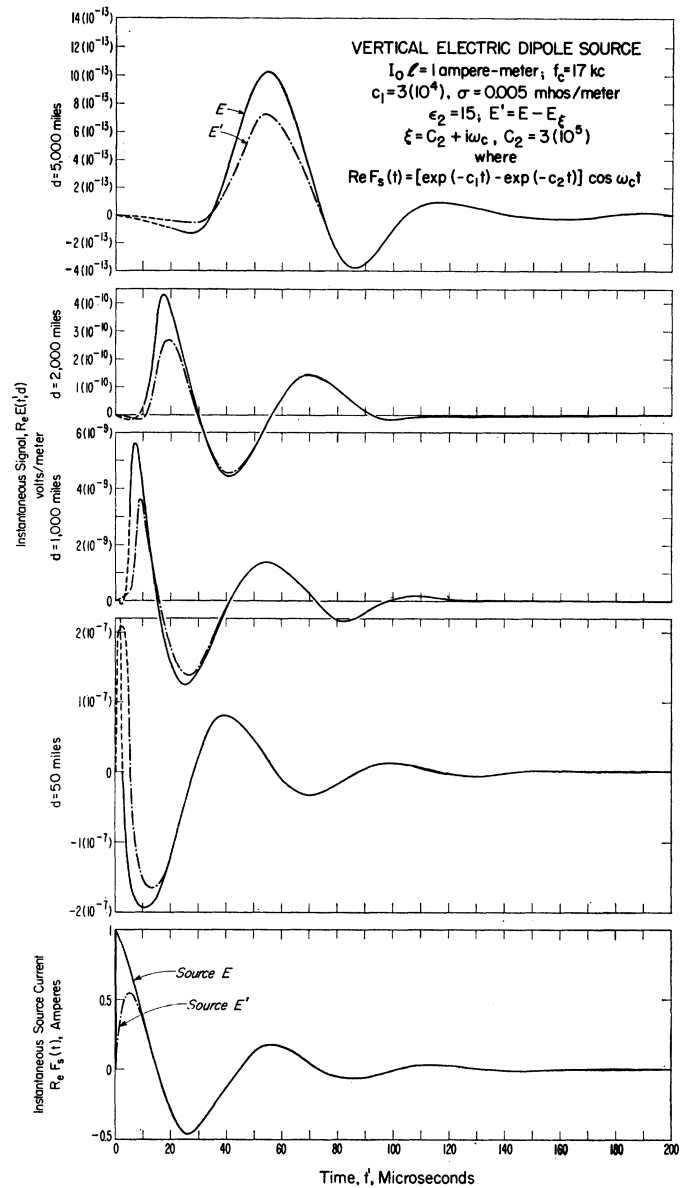


Fig. 13—Instantaneous signal and corresponding damped VLF cosine wave source current of a propagated ground wave pulse illustrating the introduction of a less abrupt initial source current.

where $A_1 = i/2$, $A_2 = -i/4$, $A_3 = -i/4$. A particular sine-squared pulse $\text{Re } E(t', d)$ is illustrated in Fig. 17 (p. 417) together with the amplitude envelope $|E(t', d)|$.

The source functions which represent natural phenomena, such as sferics (the electromagnetic radiation from thunderstorms), will not, in general, have the precise mathematical form of a damped sinusoid, impulse function or step function. Since the application of the superposition principle is not always practical, another approach to the general problem is appropriate [23], [25]. Indeed, it is quite possible to extend the theory to complicated waveforms. Consider an experiment in which the signal $\text{Re } E(t', d)$ is observed and recorded at some distance d_1 from the source. The theory is then required to predict the form of the signal recorded at some other distance d_2 . The theory is also required to determine the form of the source $F_s(t)$.

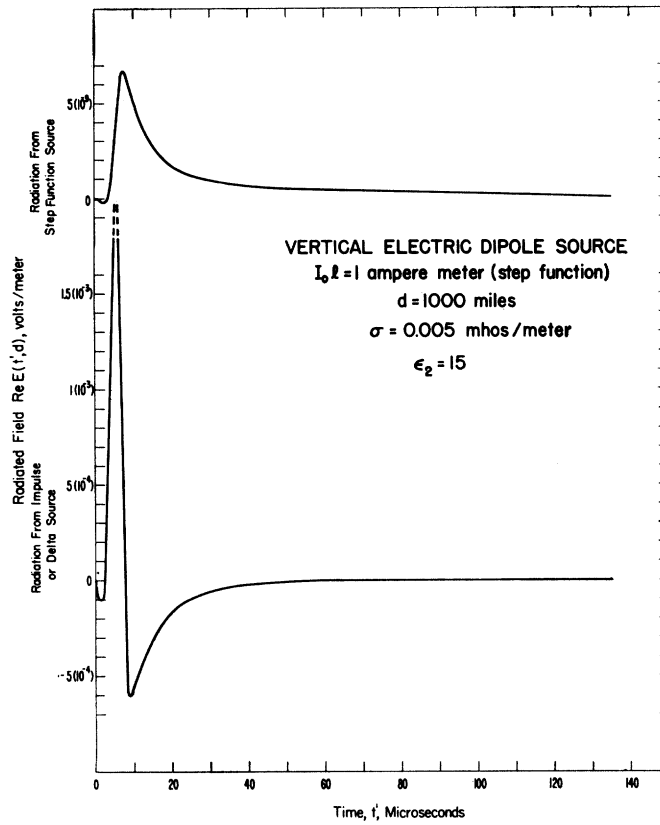


Fig. 14—The step and impulse source current radiation of the ground wave.

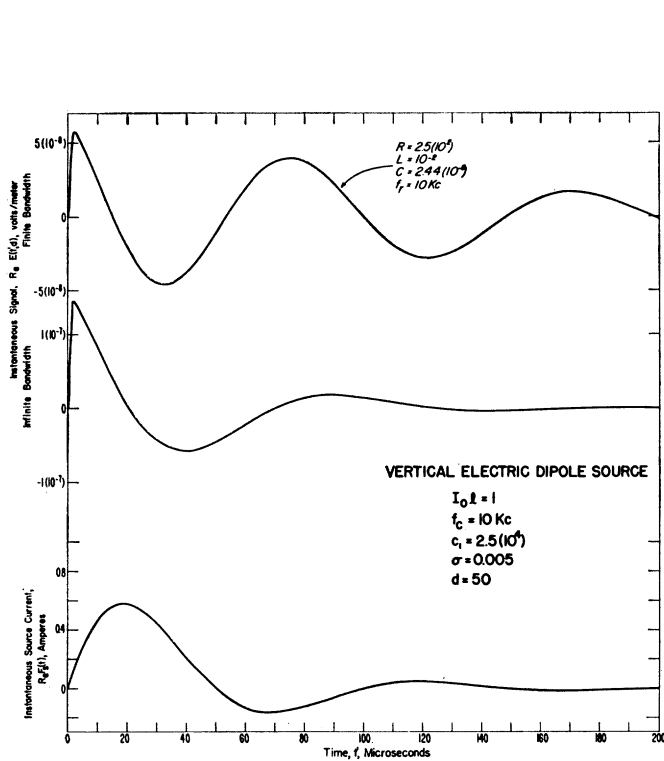


Fig. 15—Comparison of the calculation of the pulse observed through an infinite bandwidth receiver [$f_r(\omega) = 1$] with the calculation of the same pulse observed through a finite bandwidth receiver [$f_r(\omega) \neq 1$], illustrating the effect of "narrow-band" as compared with "broad-band" receiver.

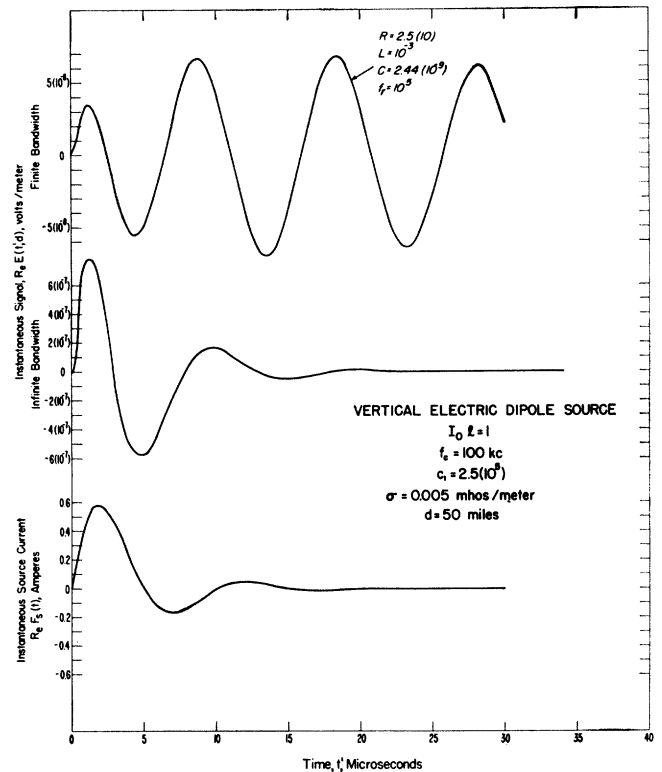


Fig. 16—Comparison of the calculation of the pulse observed through an infinite bandwidth [$f_r(\omega) = 1$] receiver with the calculation of the same pulse observed through a finite bandwidth receiver [$f_r(\omega) \neq 1$].

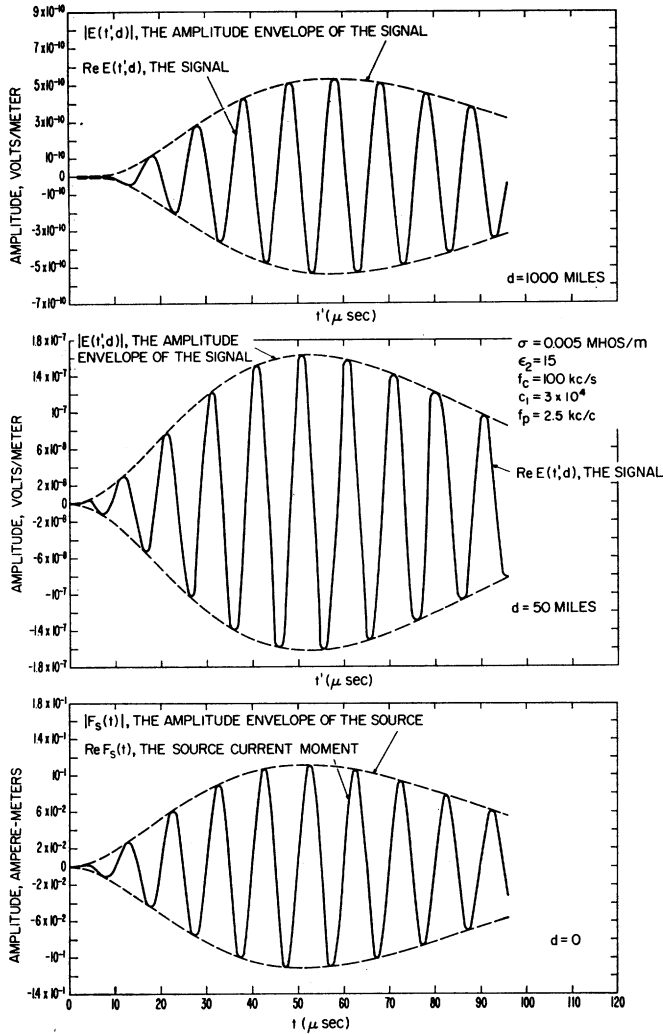


Fig. 17—The damped sine-squared pulse, illustrating synthesis of a radio-navigation system-type pulse with corresponding amplitude envelope.

The complex spectrum (48), (49) can be determined directly from the observed signal $\text{Re } E(t', d)$:

$$f_x(\omega, d) = \int_0^\infty \exp(-i\omega t') \text{Re } E(t', d) dt'. \quad (59)$$

The complex spectrum of the source $f_{x,s}(\omega)$ can then be determined

$$f_{x,s}(\omega) = \frac{f_x(\omega, d)}{E(\omega, d)}. \quad (60)$$

Since the real part of the signal $\text{Re } E(t', d)$ was employed, the source function $\text{Re } F_s(t)_\infty$ can be described

$$F_s(t) = \frac{1}{2\pi} \int_{-\infty}^\infty \exp(i\omega t) f_{x,s}(\omega) d\omega, \quad (61)$$

or

$$F_s(t) = \frac{1}{\pi} \int_0^\infty |f_{x,s}(\omega)| \{ \cos[\omega t + \phi_{x,s}(\omega)] \} d\omega, \quad (62)$$

also

$$f_x(\omega, d_2) = \frac{f_x(\omega, d_1)}{E(\omega, d_1)} E(\omega, d_2) \quad (63)$$

and

$$E(t', d_2) = \frac{1}{\pi} \int_0^\infty |f_x(\omega, d_2)| \cos[\omega t' + \phi_x(\omega, d_2)] d\omega. \quad (64)$$

Thus, with the aid of quadrature techniques [24], [26], the analysis of the detail of transient signals could be continued ad infinitum.

V. IONOSPHERIC WAVES

The essential nature of the propagation of the ionospheric waves is described by the four reflection coefficients (36), (37) $T_{ee}, T_{em}, T_{mm}, T_{me}$. These reflection coefficients can be employed in VLF mode calculations in a method developed by Wait [26]. These reflection coefficients have been employed directly in geometric-optical calculations [12]. In the latter the angle of incidence ϕ_i is real. In either case a form of polarization coupling between vertically and horizontally polarized waves external to the ionosphere can be noted. This is most obvious in the calculation of the effective reflection coefficient of the geometric-optical theory C_j (Fig. 4). Notice that each reflection from the ionosphere gives rise to both horizontal and vertical polarization as a consequence of the generation of the abnormal component, in spite of the fact that the incident wave comprises pure vertical or horizontal polarization. Thus, the abnormal component cannot be ignored in the case of vertically polarized transmitter and receiver for the ordered propagation rays, $j > 1$, i.e., $j = 2, 3, 4, \dots$. This is a form of coupling between wave polarizations quite distinct from the coupling between the magneto-ionic propagation components within the ionosphere to be described subsequently.

The evaluation of the reflection and transmission processes at the ionosphere is the most complicated part of the problem of describing the transform of the signal $E_j(\omega, d)$ for any individual time-ordered ionospheric propagation ray $j = 1, 2, 3, \dots$. The index of refraction of the ionosphere is first determined. The lower boundary of a model electron-ion plasma (Fig. 5) below which ($z < 0$) the ionization is nil ($N = 0$) or zero electron density, is considered to be the xy plane. The region above the xy plane ($z > 0$) is characterized by an electron density N and a collision frequency ν which vary with respect to altitude z . A plane wave \bar{E}_i gives

$$E_i = |\bar{E}_i| \exp\left[i\omega t - \frac{\omega}{c} \eta D\right], \quad (65)$$

where the index of refraction ($z < 0$), $\eta = \eta_0 = 1$, c is the speed of light $c \sim 3(10^8)$ m/sec and the quantity D is related to other parameters (Fig. 5) [19], [20], [27].

$$D = x \sin \phi_i \sin \phi_a + y \sin \phi_i \cos \phi_a + z \cos \phi_i, \quad (66)$$

is varying harmonically in time t at a frequency $f = \omega/2\pi$ and is assumed to be incident upon the xy plane at an angle of incidence ϕ_i and a magnetic azimuth ϕ_a is measured clockwise from the yz plane for the direction of propagation. The earth's magnetic field vector H_m ampere-turns/meter is contained in the yz plane at a dip or inclination angle I (measured from the horizontal).

A resultant wave E_t transmitted into the ionosphere model ($z > 0$) (Figs. 5 and 18) is then assumed to have the form

$$E_t = |\bar{E}_t| \exp \left[i \left(\omega t - \frac{\omega}{c} \eta D \right) \right] \quad (67)$$

where, in the plasma model,

$$\eta D = x \sin \phi_i \sin \phi_a + y \sin \phi_i \cos \phi_a + z \zeta \quad (68)$$

in which ζ is, in general, a complex number, the value of which will depend upon altitude z , $\zeta = \zeta(z)$.

The quantity ζ is determined by a simultaneous solution of Maxwell's equations

$$\begin{aligned} \bar{\nabla} \times \bar{E} + \mu_0 \frac{\partial \bar{H}}{\partial t} &= 0, \\ \bar{\nabla} \times \bar{H} - \bar{J} - \epsilon_0 \frac{\partial \bar{E}}{\partial t} &= 0, \end{aligned} \quad (69)$$

and the equation of motion of an electron (Langevin equation)

$$m \frac{d\bar{V}}{dt} + mg\bar{V} + \mu_0 e (\bar{V} \times \bar{H}_m) + e\bar{E} = 0 \quad (70)$$

with the electric field \bar{E} , the magnetic field \bar{H} (electrodynamic as distinguished from \bar{H}_m the static field of the earth), the convection current $J = -Ne\bar{V}$ for N elec-

trons per cubic meter (usually expressed as electrons/cc) with charge e , mass m , and vector velocity \bar{V} , where μ_0 and ϵ_0 are the permeability and permittivity of space, respectively. The collision frequency factor g is assumed to be a constant real number with respect to frequency; $g \sim \nu$ is the classical magneto-ionic theory.

After eliminating the vectors \bar{V} and \bar{H} , it can be concluded that field \bar{E} exists in the medium if a quartic equation in ζ is satisfied [1], [19], [20], [28],

$$a_4 \zeta^4 + a_3 \zeta^3 + a_2 \zeta^2 + a_1 \zeta + a_0 = 0 \quad (71)$$

where the coefficients of this quartic are defined in the Appendix. The roots of this equation (ζ) are quite simply related to the index of refraction of the medium η or the wave number $k = (\omega/c)\eta$, since

$$\eta^2 = \zeta^2 + \sin^2 \phi_i. \quad (72)$$

The existence of a quartic equation in the index of refraction as a direct consequence of the simultaneous solution of Maxwell's equations, (69) and the equation of motion of the electron (70) was first noted by Booker and the Booker quartic is more or less equivalent to (71).

Two pairs of roots ζ can be found [19] where each root can be identified as either ordinary or extraordinary, upgoing or downgoing magneto-ionic propagation component within the model ionosphere plasma.

Since the electron density and collision frequency can vary with respect to altitude z , a model plasma which can be deformed to fit most any measured or theoretical electron-ion profile, $N(h)$, $N(z)$, is desirable from the theoretical viewpoint to completely describe the reflection and transmission process at the ionosphere. Several approaches to this problem have been utilized by various authors such as Budden [6] and Barron [7]. The notion of a continuously varying medium

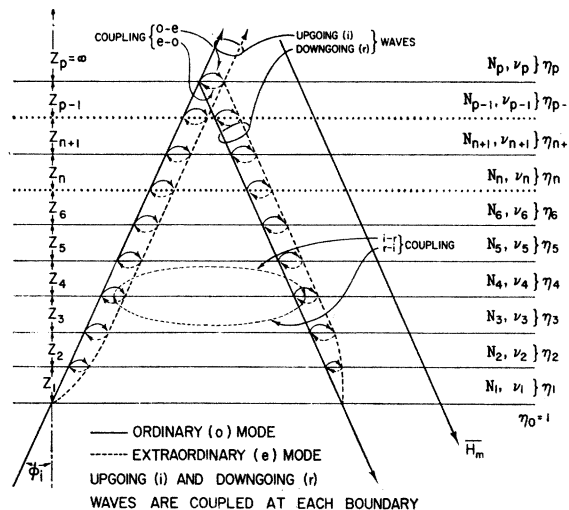


Fig. 18—Structure of the flexible plasma model, illustrating ordinary and extraordinary propagation components, coupled at the boundaries. Each slab (z_n , $n = 1, 2, 3, \dots, p$) becomes smaller as the number of slabs (p) is increased, until a stable reflection is obtained. z is always infinite where each $N = N_n$, $\nu = \nu_n$ corresponds to median values of the intervals (Z_p), respectively, of the particular profile under investigation.

has been treated by approximating the medium with one or more slabs of uniform composition as exemplified by the works of Brekhovskikh [29], Hines [30], Ferraro and Gibbon [31]. Such methods have been exploited by Johler and Harper [27], and carried to the limit, such that the number of slabs p for each calculation depends upon the computation precision required and the particular values of the electric and geometric parameters.

The detailed structure of such a flexible model is illustrated in Fig. 18 as a stack of plasma slabs of arbitrary thickness (but consistent with computation efficiency) z_n except the topmost slab of thickness $z_p = \infty$. The number of such slabs p is also quite flexible, since the notion is implied in such a model that the measured electron density-altitude, $N(h)$ or $N(z)$ profile, and collision frequency altitude, $\nu(h)$ or $\nu(z)$ profile, can be approximated to any desired accuracy by decreasing z_n and increasing p simultaneously until a stable reflection process is obtained.

A constant electron density and collision frequency with respect to altitude z is of course assumed for each slab. A set of four roots $\zeta = \zeta_n$ of (71) are found to exist in each slab. Two of the roots will exhibit a negative imaginary ($\text{Im } \zeta$ negative) corresponding to an upgoing wave ($+z$ direction, Figs. 5 and 18) and two of these roots will correspond to a positive imaginary ($\text{Im } \zeta$ positive) corresponding to a downgoing wave ($-z$ direction, Figs. 5 and 18). It is necessary to consider both upgoing and downgoing waves in the analysis of either the

reflection or transmission process at the ionosphere, except for the topmost slab, where only the upgoing waves are considered.

It is necessary to distinguish between the ordinary and extraordinary magneto-ionic components of propagation for both the upgoing and downgoing waves. This is accomplished by an examination of the form of the index of refraction function with respect to frequency and altitude (or electron density and collision frequency which varies with respect to altitude). Thus, the index of refraction η [as defined by (71), (72)] is detailed for each frequency and slab z_n , $\eta = \eta_n$. The upgoing ordinary and extraordinary $\eta_{i,o,e}^{(n)}$ and the downgoing ordinary and extraordinary $\eta_{r,o,e}^{(n)}$ function continuity is examined in detail as a function of frequency to determine, if any, the crossover points of the functions for each slab or electron density under consideration. The absolute distinction between ordinary and extraordinary magneto-ionic wave components [19], [27] remains quite arbitrary, but the analysis must be consistent between each slab and consistent within each slab for upgoing and downgoing waves.

The reflection and transmission coefficients are determined by the boundary conditions which express at the boundary of each slab the principle of continuity of the tangential \vec{E} and \vec{H} and the normal \vec{H} fields (Figs. 5 and 18) of the model plasma. These fields are equated immediately above and below each boundary and after considerable ado, a matrix equation is obtained [27],

$$\begin{bmatrix}
 a_{1,1}a_{1,2}a_{1,3}a_{1,4}a_{1,5}a_{1,6} \\
 b_{1,1}b_{1,2}b_{1,3}b_{1,4}b_{1,5}b_{1,6} \\
 c_{1,1}c_{1,2}c_{1,3}c_{1,4}c_{1,5}c_{1,6} \\
 d_{1,1}d_{1,2}d_{1,3}d_{1,4}d_{1,5}d_{1,6} \\
 \\
 a_{2,3}a_{2,4}a_{2,5}a_{2,6}a_{2,7}a_{2,8}a_{2,9}a_{2,10} \\
 b_{2,3}b_{2,4}b_{2,5}b_{2,6}b_{2,7}b_{2,8}b_{2,9}b_{2,10} \\
 c_{2,3}c_{2,4}c_{2,5}c_{2,6}c_{2,7}c_{2,8}c_{2,9}c_{2,10} \\
 d_{2,3}d_{2,4}d_{2,5}d_{2,6}d_{2,7}d_{2,8}d_{2,9}d_{2,10} \\
 \\
 a_{3,7}a_{3,8}a_{3,9}a_{3,10}a_{3,11}a_{3,12}a_{3,13}a_{3,14} \\
 b_{3,7}b_{3,8}b_{3,9}b_{3,10}b_{3,11}b_{3,12}b_{3,13}b_{3,14} \\
 c_{3,7}c_{3,8}c_{3,9}c_{3,10}c_{3,11}c_{3,12}c_{3,13}c_{3,14} \\
 d_{3,7}d_{3,8}d_{3,9}d_{3,10}d_{3,11}d_{3,12}d_{3,13}d_{3,14} \\
 \\
 \dots \\
 \dots \\
 \dots \\
 a_{p,p+4} \dots a_{p,p+9} \\
 b_{p,p+4} \dots b_{p,p+9} \\
 c_{p,p+4} \dots c_{p,p+9} \\
 d_{p,p+4} \dots d_{p,p+9}
 \end{bmatrix}
 +
 \begin{bmatrix}
 T_{em}, & T_{mm} \\
 T_{ee}, & T_{me} \\
 U_{eio}^{(1)}, & U_{mio}^{(1)} \\
 U_{eie}^{(1)}, & U_{mie}^{(1)} \\
 U_{ero}^{(1)}, & U_{mro}^{(1)} \\
 U_{ere}^{(1)}, & U_{mre}^{(1)} \\
 U_{eio}^{(2)}, & U_{mio}^{(2)} \\
 U_{eie}^{(2)}, & U_{mie}^{(2)} \\
 U_{ero}^{(2)}, & U_{mro}^{(2)} \\
 U_{ere}^{(2)}, & U_{mre}^{(2)} \\
 \dots & \dots \\
 \dots & \dots \\
 U_{eio}^{(p-1)}, & U_{mio}^{(p-1)} \\
 U_{eie}^{(p-1)}, & U_{mie}^{(p-1)} \\
 U_{ero}^{(p-1)}, & U_{mro}^{(p-1)} \\
 U_{ere}^{(p-1)}, & U_{mre}^{(p-1)} \\
 U_{eio}^{(p)}, & U_{mio}^{(p)} \\
 U_{eie}^{(p)}, & U_{mie}^{(p)}
 \end{bmatrix}
 = 0, \quad (73)$$

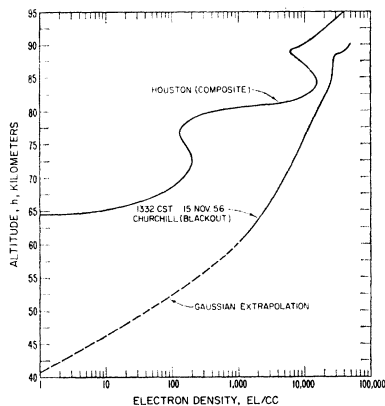


Fig. 19—Electron density-altitude $[N(h)$ or $\nu(z)]$ (quiescent and disturbed) profiles.

where the elements of the matrix $a_{1,1} \dots$ are defined in the Appendix.

The upgoing ordinary and extraordinary and the downgoing ordinary and extraordinary magneto-ionic components of propagation are coupled within the ionosphere (Fig. 18) as a result of the introduction of the boundary conditions described in concise form in the matrix equation (73). Thus, at the upper and lower boundary of each slab, energy is transferred between the four magneto-ionic components of propagation [four roots of the quartic equation (71)]. This type of coupling is distinct from the coupling of the polarization components, external to the ionosphere described previously [beginning of Section V—see also Fig. 4 and (36)].

The continuously stratified technique can be illustrated by evaluating reflections from an ionosphere model determined by actual measured profiles of electron density (Fig. 19) and collision frequency (Fig. 20). A typical daytime-room profile $N(h)$ presented by Waynick [32] (Fig. 19) and a corresponding disturbed profile of Seddon and Jackson [33], indicative of the intensity of ionization during a local auroral zone ionosonde blackout, were selected for purposes of illustrating application of the described continuous stratification techniques. The region of the ionosphere on the latter curve, below 1000 electrons/cc, was represented (dashed curve, Fig. 19) with a Gaussian distribution [6],

$$N = N_{\max} \exp [-(z - z_{\max})^2/k'],$$

where the constants N_{\max} , z_{\max} , and k' were determined by the measured profile >1000 electrons/cc. In particular, $N_{\max} = 26,000$, $z_{\max} = 85,000$, $k' = 1.92 (10^8)$.

The Nicolet/3 collision frequency [34], [35] was employed in this analysis. These collision frequencies are applicable to the classical magneto-ionic theory employing the approximation $g \sim \nu$ [27], [36] in the equation of motion of the electron (70).

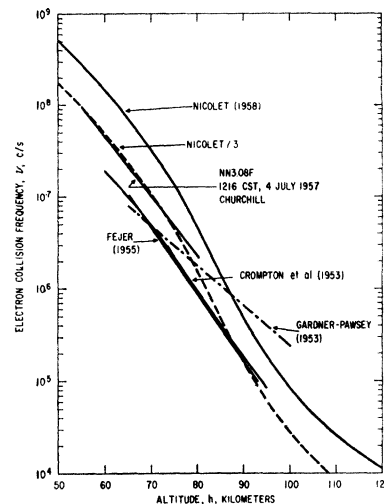


Fig. 20—Collision frequency-altitude $[\nu(h)$ or $\nu(z)]$ profiles (Nicolet/3 was employed in calculations).

The reflection coefficients T_{ee} , T_{em} , T_{me} , and T_{mm} were evaluated (Figs. 21–28, pp. 421–422). The reflection coefficients for the quiescent profiles are illustrated in Figs. 19–25. The disturbed profiles reflection coefficients are illustrated in Figs. 26–28.

The reflection coefficients $|T_{ee}|$, $|T_{mm}|$ show a steady decrease in amplitude as the frequency is increased. A small perceptible rise is noted near the gyrofrequency, however. This was a result of the approximation $g \sim \nu$ [27] and the assumed model, whereas the use of a complex collision frequency g could exhibit higher attenuation near the gyrofrequency. Such a complex collision frequency can be deduced from the work of Phelps [36], Molmud [37], Jancel and Kahan [38], where a collision frequency $\nu = \nu(u)$ proportional to the electron energy or temperature is derived. Johler and Harper [27] have introduced electron collisions proportional to energy as a modification of the coefficients of the quartic equation (71). This, of course, introduces some changes in the detail of the reflection coefficients, but the general form of the reflection coefficients of the classical magneto-ionic theory remains unaltered at LF/VLF.

The magnitude of the abnormal components $|T_{em}|$, $|T_{me}|$ also shows a decrement as a function of frequency. These components are quite small for the assumed model (<0.1 at 10 kc, for example). The corresponding disturbed blackout reflection coefficients imply a slight change in the angle of incidence ϕ ; as a result of a lowering of the ionosphere. However, the principal cause of change as a result of this profile is, nevertheless, the redistribution of the electron density-altitude profile. It is interesting to note an increased attenuation at the higher frequencies 100 kc to 1000 kc. However, the high attenuation or total ionosonde blackout which characterizes high frequencies does not seem to exist at LF. Indeed, an enhancement in the field is anticipated from this profile at VLF (<30 kc).

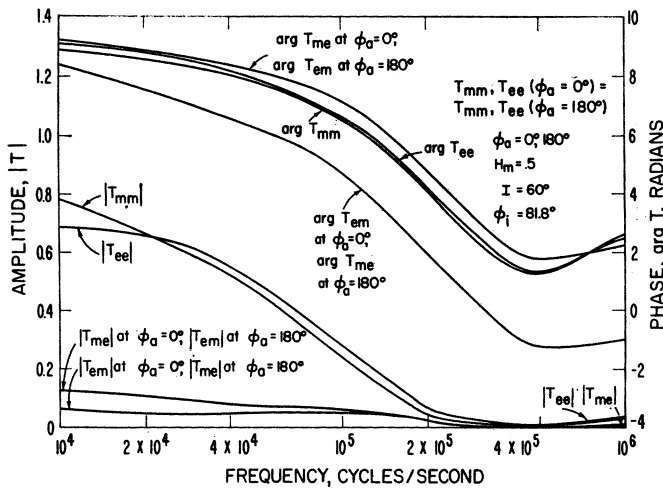


Fig. 21—Reflection coefficients (amplitude and phase) of the lower ionosphere for LF's, illustrating the frequency dependence of the classical magneto-ionic theory ($\phi_a = 0, 180^\circ$).

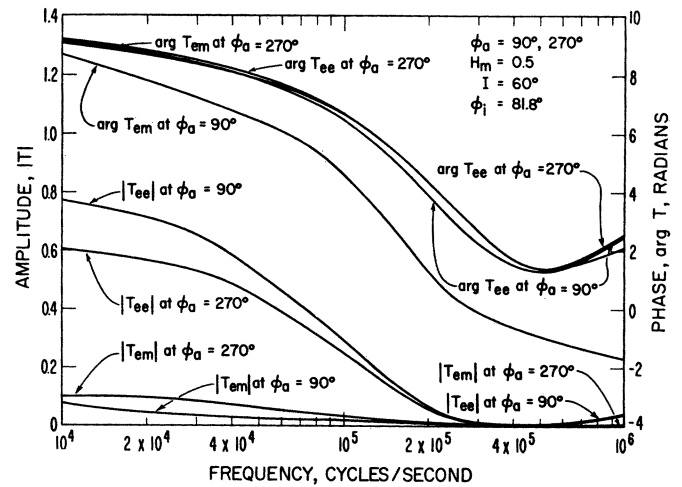


Fig. 22—Reflection coefficients (amplitude and phase) of the lower ionosphere for LF's, illustrating the frequency dependence of the classical magneto-ionic theory ($\phi_a = 90^\circ, 270^\circ$), vertical polarization (T_{ee}, T_{em}).

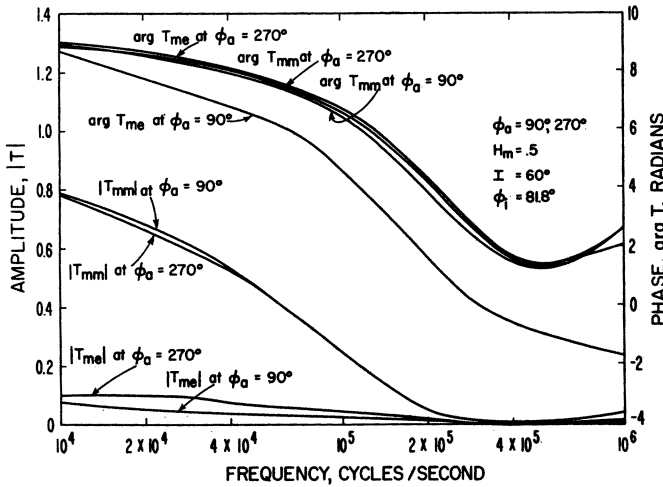


Fig. 23—Reflection coefficients (amplitude and phase) of the lower ionosphere for LF's, illustrating the frequency dependence of the classical magneto-ionic theory ($\phi_a = 90^\circ, 270^\circ$), horizontal polarization (T_{mm}, T_{me}).

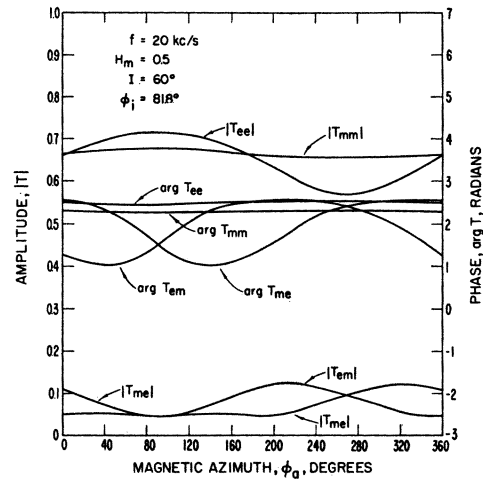


Fig. 24—Reflection coefficients (amplitude and phase) of the lower ionosphere for LF's, illustrating the action of the Lorentzian force (earth's magnetic field) in the classical magneto-ionic theory ($f = 20$ kc).

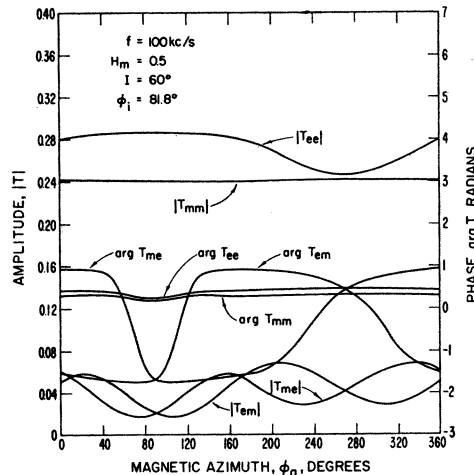


Fig. 25—Reflection coefficients (amplitude and phase) of the lower ionosphere for LF's, illustrating the action of the Lorentzian force (earth's magnetic field) in the classical magneto-ionic theory ($f = 100$ kc).

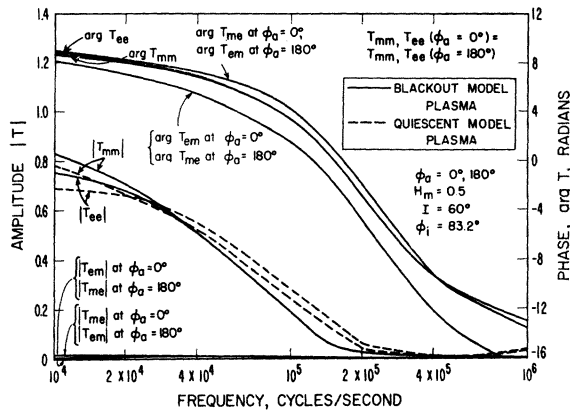


Fig. 26—Reflection coefficients (amplitude and phase) of the lower ionosphere for LF's during disturbed conditions, illustrating the frequency dependence of the classical magneto-ionic theory. $|T_{ee}|$ and $|T_{mm}|$ are also illustrated for comparison with the quiescent conditions (see Figs. 21–25 for complete reflection coefficients). ($\phi_a = 0, 180^\circ$.)

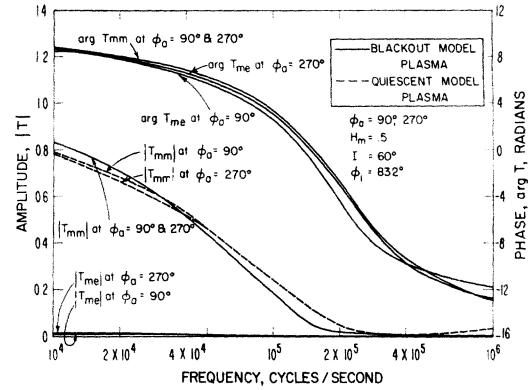


Fig. 27—Reflection coefficients (amplitude and phase) of the lower ionosphere for LF's during disturbed conditions, illustrating the frequency dependence of the classical magneto-ionic theory. $|T_{ee}|$ and $|T_{mm}|$ are also illustrated for comparison with quiescent conditions (see Figs. 21–25 for complete reflection coefficients). ($\phi_a = 90^\circ, 270^\circ$, vertical polarization T_{ee}, T_{em} .)

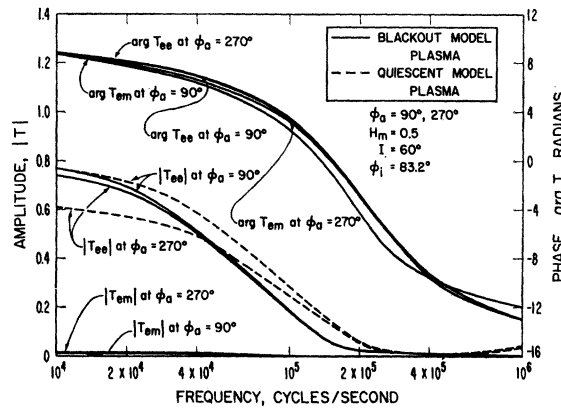


Fig. 28—Reflection coefficients (amplitude and phase) of the lower ionosphere for LF's during disturbed conditions, illustrating the frequency dependence of the classical magneto-ionic theory. $|T_{ee}|$ and $|T_{mm}|$ are also illustrated for comparison with quiescent conditions (see Figs. 21–25 for complete reflection coefficients). ($\phi_a = 90^\circ, 270^\circ$, horizontal polarization, T_{mm}, T_{mc} .)

The effect of the Lorentzian force, $\mu_0 e(\bar{V} \times \bar{H}_m)$, [see (70)], or the action of the earth's magnetic field on the reflection process is also illustrated in Figs. 24 and 25. The reflection coefficients are illustrated here as a function of magnetic azimuth ϕ_a (Fig. 5). Note the propagation into the west, $\phi_a = 270^\circ$, shows a smaller reflection coefficient than the propagation into the east, $\phi_a = 90^\circ$, for the particular example illustrated. This seems to be quite generally valid for grazing incidence type transmission, $\phi_i \sim 82^\circ$. This clearly indicates a nonreciprocity in the transmission, *i.e.*, the interchange of transmitter and receiver would not produce the same field.

Although the ionosphere reflections are quite intricate, it is quite feasible to evaluate the field of each ionospheric propagation ray, $E_j(\omega, d)$, (7), (8) or the total field, $E(\omega, d)$. The application of the transformation techniques (1)–(4), (39), (41)–(46) can then be applied to particular signal sources (as was illustrated

for the ground wave, Section IV), $F_s(t)$. The propagated ionospheric signals $E_j(t', d)$ will thus be determined.

VI. CONCLUSIONS

Low frequencies exhibit properties which are quite favorable to high reliability and precision radio navigation-timing. In particular, the ground wave signal is especially favorable at distances less than 2000 statute miles (3200 km), *i.e.*, the pulse type transmissions resolve or sort out the individual propagation rays. At greater distances the signals propagated via ionospheric propagation rays also exhibit favorable properties, provided again the individual ionospheric propagation rays are sorted in the time domain. The detailed investigation of these properties is now required as a result of the economic and scientific importance of the navigation timing and communications systems now operating at LF.

APPENDIX

The coefficients of the quartic equation (71) are

$$a_0 = (a^2 - 1)^2 \left[1 - \frac{s}{s^2 - h^2} \right] + (a^2 - 1) \left[\frac{1}{s} + \frac{s - 2}{s^2 - h^2} + \frac{a_L^2 h_T^2}{s(s^2 - h^2)} + \frac{s - 1}{s(s^2 - h^2)} \right], \quad (74)$$

$$a_1 = 2 \frac{h_L h_T a_L}{s(s^2 - h^2)} (a^2 - 1), \quad (75)$$

$$a_2 = \left\{ 2 \left[1 - \frac{s}{s^2 - h^2} \right] + \frac{h_L^2}{s(s^2 - h^2)} \right\} (a^2 - 1) + \frac{h_T^2 a_L^2}{s(s^2 - h^2)} + \frac{s - 2}{s^2 - h^2} + \frac{1}{s}, \quad (76)$$

$$a_3 = 2 \frac{h_L h_T a_L}{s(s^2 - h^2)} = -a_1 \sec^2 \phi_i = -a_1 / (1 - a^2), \quad (77)$$

$$a_4 = 1 - \frac{s^2 - h_L^2}{s(s^2 - h^2)}, \quad (78)$$

$$s = \frac{\omega^2}{\omega_N^2} \left[1 - i \frac{\nu}{\omega} \right], \quad (79)$$

where (Fig. 18) $\nu = \nu_n$, the collision frequency of the particular altitude n under investigation is

$$h = \frac{\omega_H \omega}{\omega_N^2}, \quad (80)$$

$$h_L = -h \sin I, \quad (81)$$

$$h_T = h \cos I, \quad (82)$$

$$a_L = \sin \phi_i \cos \phi_a, \quad a_T = \sin \phi_i \sin \phi_a, \quad (83)$$

$$a = \sin \phi_i, \quad (84)$$

$$\omega_N^2 = Ne^2 / \kappa m, \quad (85)$$

and the electron density of the particular slab n (Fig. 18) under investigation is

$$\omega_H = \mu_0 e H_m / m, \quad (86)$$

$$\kappa = 1/c^2 \mu_0 = \epsilon_0. \quad (87)$$

The elements of the matrix equation (73) are defined:

$$a_{1,1} = \cos \phi_a$$

$$a_{1,2} = -\cos \phi_i \sin \phi_a$$

$$a_{1,3} = -Q_{io}^{(1)}$$

$$a_{1,4} = -Q_{ie}^{(1)}$$

$$a_{1,5} = -Q_{ro}^{(1)}$$

$$a_{1,6} = -Q_{re}^{(1)}$$

$$a_{2,3} = -a_{1,3} \exp \left[-i \frac{\omega}{c} z_1 \zeta_{io}^{(1)} \right]$$

$$a_{2,4} = -a_{1,4} \exp \left[-i \frac{\omega}{c} z_1 \zeta_{ie}^{(1)} \right]$$

$$a_{2,5} = -a_{1,5} \exp \left[-i \frac{\omega}{c} z_1 \zeta_{ro}^{(1)} \right]$$

$$b_{1,1} = -\sin \phi_a$$

$$b_{1,2} = -\cos \phi_i \cos \phi_a$$

$$b_{1,3} = -1$$

$$b_{1,4} = -1$$

$$b_{1,5} = -1$$

$$b_{1,6} = -1$$

$$b_{2,3} = \exp \left[-i \frac{\omega}{c} z_1 \zeta_{io}^{(1)} \right]$$

$$b_{2,4} = \exp \left[-i \frac{\omega}{c} z_1 \zeta_{ie}^{(1)} \right]$$

$$b_{2,5} = \exp \left[-i \frac{\omega}{c} z_1 \zeta_{ro}^{(1)} \right]$$

$$\begin{aligned}
a_{2,6} &= -a_{1,6} \exp \left[-i \frac{\omega}{c} z_1 \zeta_{re}^{(1)} \right] & b_{2,6} &= \exp \left[-i \frac{\omega}{c} z_1 \zeta_{re}^{(1)} \right] \\
a_{2,7} &= -Q_{io}^{(2)} & b_{2,7} &= -1 \\
a_{2,8} &= -Q_{ie}^{(2)} & b_{2,8} &= -1 \\
a_{2,9} &= -Q_{ro}^{(2)} & b_{2,9} &= -1 \\
a_{2,10} &= -Q_{re}^{(2)} & b_{2,10} &= -1 \\
a_{3,7} &= -a_{2,7} \exp \left[-i \frac{\omega}{c} z_2 \zeta_{io}^{(2)} \right] & b_{3,7} &= \exp \left[-i \frac{\omega}{c} z_2 \zeta_{io}^{(2)} \right] \\
a_{3,8} &= -a_{2,8} \exp \left[-i \frac{\omega}{c} z_2 \zeta_{ie}^{(2)} \right] & b_{3,8} &= \exp \left[-i \frac{\omega}{c} z_2 \zeta_{ie}^{(2)} \right] \\
a_{3,9} &= -a_{2,9} \exp \left[-i \frac{\omega}{c} z_2 \zeta_{ro}^{(2)} \right] & b_{3,9} &= \exp \left[-i \frac{\omega}{c} z_2 \zeta_{ro}^{(2)} \right] \\
a_{3,10} &= -a_{2,10} \exp \left[-i \frac{\omega}{c} z_2 \zeta_{re}^{(2)} \right] & b_{3,10} &= \exp \left[-i \frac{\omega}{c} z_2 \zeta_{re}^{(2)} \right] \\
a_{3,11} &= -Q_{io}^{(3)} & b_{3,11} &= -1 \\
a_{3,12} &= -Q_{ic}^{(3)} & b_{3,12} &= -1 \\
a_{3,13} &= -Q_{ro}^{(3)} & b_{3,13} &= -1 \\
a_{3,14} &= -Q_{re}^{(3)} & b_{3,14} &= -1 \\
&\dots & & \dots \\
a_{p,p+4} &= -a_{p-1,p+4} \exp \left[-i \frac{\omega}{c} z_{p-1} \zeta_{io}^{(p-1)} \right] & b_{p,p+4} &= \exp \left[-i \frac{\omega}{c} z_{p-1} \zeta_{io}^{(p-1)} \right] \\
a_{p,p+9} &= -Q_{ic}^{(p)} & b_{p,p+9} &= -1 \\
c_{1,1} &= -\cos \phi_i \sin \phi_a & d_{1,1} &= -\cos \phi_i \cos \phi_a \\
c_{1,2} &= -\cos \phi_a & d_{1,2} &= \sin \phi_a \\
c_{1,3} &= -[a_L P_{io}^{(1)} - \zeta_{io}^{(1)}] & d_{1,3} &= -[\zeta_{io}^{(1)} Q_{io}^{(1)} - a_T P_{io}^{(1)}] \\
c_{1,4} &= -[a_L P_{ic}^{(1)} - \zeta_{ie}^{(1)}] & d_{1,4} &= -[\zeta_{ie}^{(1)} Q_{ie}^{(1)} - a_T P_{ie}^{(1)}] \\
c_{1,5} &= -[a_L P_{ro}^{(1)} - \zeta_{ro}^{(1)}] & d_{1,5} &= -[\zeta_{ro}^{(1)} Q_{ro}^{(1)} - a_T P_{ro}^{(1)}] \\
c_{1,6} &= -[a_L P_{re}^{(1)} - \zeta_{re}^{(1)}] & d_{1,6} &= -[\zeta_{re}^{(1)} Q_{re}^{(1)} - a_T P_{re}^{(1)}] \\
c_{2,3} &= -c_{1,3} \exp \left[-i \frac{\omega}{c} z_1 \zeta_{io}^{(1)} \right] & d_{2,3} &= -d_{1,3} \exp \left[-i \frac{\omega}{c} z_1 \zeta_{io}^{(1)} \right] \\
c_{2,4} &= -c_{1,4} \exp \left[-i \frac{\omega}{c} z_1 \zeta_{ie}^{(1)} \right] & d_{2,4} &= -d_{1,4} \exp \left[-i \frac{\omega}{c} z_1 \zeta_{ie}^{(1)} \right] \\
c_{2,5} &= -c_{1,5} \exp \left[-i \frac{\omega}{c} z_1 \zeta_{ro}^{(1)} \right] & d_{2,5} &= -d_{1,5} \exp \left[-i \frac{\omega}{c} z_1 \zeta_{ro}^{(1)} \right] \\
c_{2,6} &= -c_{1,6} \exp \left[-i \frac{\omega}{c} z_1 \zeta_{re}^{(1)} \right] & d_{2,6} &= -d_{1,6} \exp \left[-i \frac{\omega}{c} z_1 \zeta_{re}^{(1)} \right] \\
c_{2,7} &= -[a_L P_{io}^{(2)} - \zeta_{io}^{(2)}] & d_{2,7} &= -[\zeta_{io}^{(2)} Q_{io}^{(2)} - a_T P_{io}^{(2)}] \\
c_{2,8} &= -[a_L P_{ie}^{(2)} - \zeta_{ie}^{(2)}] & d_{2,8} &= -[\zeta_{ie}^{(2)} Q_{ie}^{(2)} - a_T P_{ie}^{(2)}] \\
c_{2,9} &= -[a_L P_{ro}^{(2)} - \zeta_{ro}^{(2)}] & d_{2,9} &= -[\zeta_{ro}^{(2)} Q_{ro}^{(2)} - a_T P_{ro}^{(2)}] \\
c_{2,10} &= -[a_L P_{re}^{(2)} - \zeta_{re}^{(2)}] & d_{2,10} &= -[\zeta_{ie}^{(2)} Q_{ie}^{(2)} - a_T P_{re}^{(2)}]
\end{aligned}$$

$$\begin{aligned}
 c_{3,7} &= -c_{2,7} \exp \left[-i \frac{\omega}{c} z_2 \zeta_{io}^{(2)} \right] & d_{3,7} &= -d_{2,7} \exp \left[-i \frac{\omega}{c} z_2 \zeta_{io}^{(2)} \right] \\
 c_{3,8} &= -c_{2,8} \exp \left[-i \frac{\omega}{c} z_2 \zeta_{ie}^{(2)} \right] & d_{3,8} &= -d_{2,8} \exp \left[-i \frac{\omega}{c} z_2 \zeta_{ie}^{(2)} \right] \\
 c_{3,9} &= -c_{2,9} \exp \left[-i \frac{\omega}{c} z_2 \zeta_{ro}^{(2)} \right] & d_{3,9} &= -d_{2,9} \exp \left[-i \frac{\omega}{c} z_2 \zeta_{ro}^{(2)} \right] \\
 c_{3,10} &= -c_{2,10} \exp \left[-i \frac{\omega}{c} z_2 \zeta_{re}^{(2)} \right] & d_{3,10} &= -d_{2,10} \exp \left[-i \frac{\omega}{c} z_2 \zeta_{re}^{(2)} \right] \\
 c_{3,11} &= -[a_L P_{io}^{(3)} - \zeta_{io}^{(3)}] & d_{3,11} &= -[\zeta_{io}^{(3)} Q_{io}^{(3)} - a_T P_{io}^{(3)}] \\
 c_{3,12} &= -[a_L P_{ie}^{(3)} - \zeta_{ie}^{(3)}] & d_{3,12} &= -[\zeta_{ie}^{(3)} Q_{ie}^{(3)} - a_T P_{ie}^{(3)}] \\
 c_{3,13} &= -[a_L P_{ro}^{(3)} - \zeta_{ro}^{(3)}] & d_{3,13} &= -[\zeta_{ro}^{(3)} Q_{ro}^{(3)} - a_T P_{ro}^{(3)}] \\
 c_{3,14} &= -[a_L P_{re}^{(3)} - \zeta_{re}^{(3)}] & d_{3,14} &= -[\zeta_{re}^{(3)} Q_{re}^{(3)} - a_T P_{re}^{(3)}] \\
 &\dots & &\dots \\
 c_{p,p+4} &= -c_{p-1,p+4} \exp \left[-i \frac{\omega}{c} z_{p-1} \zeta_{io}^{(p-1)} \right] & d_{p,p+4} &= -d_{p-1,p+4} \exp \left[-i \frac{\omega}{c} z_{p-1} \zeta_{io}^{(p-1)} \right] \\
 c_{p,p+9} &= -[a_L P_{ie}^{(p)} - \zeta_{ie}^{(p)}] & d_{p,p+9} &= -[\zeta_{ie}^{(p)} Q_{ie}^{(p)} - a_T P_{ie}^{(p)}] \\
 \\
 a_{oe} &= \cos \phi_i \sin \phi_a \\
 b_{oe} &= \cos \phi_i \cos \phi_a \\
 c_{oe} &= -\cos \phi_a \\
 d_{oe} &= \sin \phi_a \\
 a_{om} &= \cos \phi_a \\
 b_{om} &= -\sin \phi_a \\
 c_{om} &= \cos \phi_i \sin \phi_a \\
 d_{om} &= \cos \phi_i \cos \phi_a
 \end{aligned}$$

and

$$P = E_z/E_y, \quad Q = E_x/E_y.$$

Both transmission coefficients U and reflection coefficients T previously introduced (37) are determined by the matrix. The U 's are defined as

$$\begin{aligned}
 U_{eio}^{(n)} &= \frac{E_{yio}^{(n)}}{E_{y'i}} & U_{ero}^{(n)} &= \frac{E_{yro}^{(n)}}{E_{y'i}} \\
 U_{mio}^{(n)} &= \frac{E_{yio}^{(n)}}{E_{x'i}} & U_{mro}^{(n)} &= \frac{E_{yro}^{(n)}}{E_{x'i}} \\
 U_{eie}^{(n)} &= \frac{E_{yie}^{(n)}}{E_{y'i}} & U_{ere}^{(n)} &= \frac{E_{yre}^{(n)}}{E_{y'i}} \\
 U_{mie}^{(n)} &= \frac{E_{yie}^{(n)}}{E_{x'i}} & U_{mre}^{(n)} &= \frac{E_{yre}^{(n)}}{E_{x'i}}.
 \end{aligned} \tag{88}$$

The analytic expressions for the complex numbers $P_{io}^{(n)}$, $P_{ie}^{(n)}$, $P_{ro}^{(n)}$, $P_{re}^{(n)}$, $Q_{io}^{(n)}$, $Q_{ie}^{(n)}$, $Q_{ro}^{(n)}$, $Q_{er}^{(n)}$ can be derived from the definitions by a simultaneous solution of Maxwell's equation (69) and the equation of motion of the electron (70) with the following result:

$$P = \frac{-\left[a_L \zeta + \frac{h_T h_L}{s(s^2 - h^2)} \right] \left[1 - a_L^2 - \zeta^2 - \frac{s}{s^2 - h^2} \right] + \left[a_L a_T - i \frac{h_L}{s^2 - h^2} \right] \left[a_T \zeta - i \frac{h_T}{s^2 - h^2} \right]}{\left[1 - a^2 - \frac{s^2 - h_L^2}{s(s^2 - h^2)} \right] \left[1 - a_L^2 - \zeta^2 - \frac{s}{s^2 - h^2} \right] - \left[a_T \zeta + i \frac{h_T}{s^2 - h^2} \right] \left[a_T \zeta - i \frac{h_T}{s^2 - h^2} \right]}, \quad (89)$$

$$Q = \frac{-\left[1 - a^2 - \frac{s^2 - h_L^2}{s(s^2 - h^2)} \right] \left[a_L a_T - i \frac{h_L}{s^2 - h^2} \right] + \left[a_T \zeta + i \frac{h_T}{s^2 - h^2} \right] \left[a_L \zeta + \frac{h_L h_T}{s(s^2 - h^2)} \right]}{\left[1 - a^2 - \frac{s^2 - h_L^2}{s(s^2 - h^2)} \right] \left[1 - a_L^2 - \zeta^2 - \frac{s}{s^2 - h^2} \right] - \left[a_T \zeta + i \frac{h_T}{s^2 - h^2} \right] \left[a_T \zeta - i \frac{h_T}{s^2 - h^2} \right]}, \quad (90)$$

where the particular slab (Fig. 18) $n=1, 2, 3, \dots, p-1, p$ under consideration is designated by the notation $\zeta = \zeta^{(n)}$, $P = P^{(n)}$, $Q = Q^{(n)}$, and $io, ie, ro,$ and re refer to the four roots of the quartic in ζ for upgoing, downgoing, ordinary, and extraordinary waves, respectively, in the particular part z_n of the electron-ion plasma under consideration.

The factor $F_j^{t,r}$ can be written [12]

$$F_j^{t,r} = (\pi)^{-1/2} \exp[-ik_1 a \theta'] \cdot \left\{ \int_0^\infty \frac{\exp[-i(k_1 a/2)^{1/3} \theta' \alpha]}{W_1'(\alpha) - qW_1(\alpha)} d\alpha - \int_0^\infty \frac{\exp[-i(k_1 a/2)^{1/3} \theta' \alpha' - i2\pi/3]}{W_1'(\alpha') - qW_1(\alpha')} d\alpha' \right\},$$

where $\alpha' = \alpha \exp[-i2\pi/3]$ and

$$W_1(\alpha') = -i\sqrt{\pi/3} (\alpha)^{1/2} H_{1/3}^{(2)} \left[\frac{2}{3} i \alpha^{3/2} \right]$$

$$W_1'(\alpha') = \sqrt{\pi/3} \alpha H_{2/3}^{(2)} \left[\frac{2}{3} i \alpha^{3/2} \right],$$

where α is a positive real number.

The following explicit form for the equation $F_j^{t,r}$ has been suggested [39]:

$$F_j^{t,r} = (\pi)^{-1/2} \exp[-ik_1 a \theta'] \cdot \left\{ \int_0^\infty \frac{\exp[-i(k_1 a/2)^{1/3} \theta' \alpha]}{W_1'(\alpha) - qW_1(\alpha)} d\alpha + \int_0^\infty \frac{\exp\left[-\frac{(\sqrt{3-i})}{2} (k_1 a/2)^{1/3} \theta' \alpha\right]}{W_2'(\alpha) - q \exp[-i2\pi/3] W_2(\alpha)} d\alpha \right\},$$

where $W_2(\alpha)$ and $W_2'(\alpha)$ are airy integral functions appropriate to the rotation $\alpha' = \alpha \exp(-2\pi i/3)$.

REFERENCES

- [1] H. Bremmer, "Terrestrial Radio Waves—Theory of Propagation," Elsevier Publishing Co., New York, N. Y.; 1949.
- [2] J. R. Wait, "Diffraction theory for LF sky-wave propagation," *J. Geophys. Res.*, vol. 66, 1713–1730; June, 1961.
- [3] G. Hefley, "Timing potentials of Loran-C," *Signal J. Armed Forces Commun. and Electronics Assoc.*, vol. 15, pp. 45–47; February, 1961.
- [4] W. P. Frantz, W. N. Dean, and R. C. Frank, "A precision multi-purpose radio navigation system," 1957 IRE CONVENTION RECORD, pt. 8, pp. 79–120.
- [5] J. S. Belrose, W. L. Hatton, C. A. McKerrow, and R. S. Thain, "The engineering of communication systems for low radio-frequencies," *PROC. IRE*, vol. 47, pp. 661–680; May, 1959.
- [6] K. G. Budden, "The numerical solution of the differential equations governing the reflection of long radio waves from the ionosphere, II," *Proc. Roy. Soc. (London) A*, Phil. Trans., vol. 248, pp. 45–72; 1955–1956.
- [7] D. W. Barron, "The numerical solution of differential equations governing the reflexion of long radio waves from the ionosphere, IV," *Proc. Roy. Soc. (London), A*, vol. 260, pp. 393–408; March, 1961.
- [8] H. Hertz, "Die Kräfte Elektrischer Schwingungen Behnadelt nach der Maxwell'schen Theorie," *Ann. Phys. Chem. (Leipzig)*, vol. 36, pp. 1–22; 1889.
- [9] H. A. Lorentz, "The Theory of Electrons and its Applications to the Phenomena of Light and Radiant Heat," G. E. Stechert and Co., New York, N. Y.; 1906.
- [10] A. Sommerfeld, "Über die Fortpflanzung des Lichtes in Dispergierenden Medien," *Ann. Phys.*, vol. 44, pp. 177–302; October, 1914.
- [11] L. Brillouin, "Über die Fortpflanzung des Lichtes in Dispergierenden Medien," *Ann. Phys.*, vol. 44, pp. 203–240; October, 1914.
- [12] J. R. Johler, "On the analysis of LF ionospheric radio propagation phenomena," *J. Res. NBS*, vol. 65D, pp. 507–529; September–October, 1961.
- [13] J. R. Johler, W. J. Kellar, and L. C. Walters, "Phase of the Low Radiofrequency Ground Wave," U. S. Gov. Printing Office, Washington, D. C., NBS Circular 573; June, 1956.
- [14] J. R. Wait, "Diffractive corrections to the geometrical optics of low frequency propagation," in "Electromagnetic Wave Propagation," Academic Press, London, Eng.; 1960.
- [15] J. R. Wait and A. M. Conda, "Pattern of an antenna on a curved lossy surface," *IRE TRANS. ON ANTENNAS AND PROPAGATION*, vol. AP-6, pp. 348–359; October, 1958.
- [16] J. R. Johler, L. C. Walters, and C. M. Lilley, "Low- and Very Low-Radiofrequency Tables of Ground Wave Parameters for the Spherical Earth Theory: the Roots of Riccati's Differential Equation," U. S. Dept. of Commerce, Office Tech. Services, Washington, D. C., NBS Tech. Note No. 7, PB-151366; February, 1959.
- [17] H. H. Howe, "Note on the solution of Riccati's differential equation," *J. Res. NBS*, vol. 64B, pp. 95–97; April–June, 1960.
- [18] L. C. Walters and J. R. Johler, "On the diffraction of spherical waves in the vicinity of a sphere," *J. Res. NBS*, vol. 66D, pp. 101–106; January–February, 1962.
- [19] J. R. Johler and L. C. Walters, "On the theory of reflection of low- and very low-radiofrequency waves from the ionosphere," *J. Res. NBS*, vol. 64D, pp. 259–285; May–June, 1960.
- [20] J. R. Johler, "Magneto-ionic propagation phenomena in low- and very low-radiofrequency waves reflected by the ionosphere," *J. Res. NBS*, vol. 65D, pp. 53–65; January–February, 1961.
- [21] J. R. Johler, "On LF ionospheric phenomena in radio navigation

- systems," presented at Avionics Panel Meeting of the Advisory Group of Aeronautical Res. Dev. (AGARD), Istanbul, Turkey; October 3-8, 1960 (to be published, Pergamon Press, 1961-62).
- [22] J. R. Johler, "A Note on the Propagation of Certain LF Pulses Utilized in a Radio Navigation System," U. S. Dept. of Commerce, Office of Tech. Services, Washington, D. C., NBS Tech. Note No. 118, PB-161619; September, 1961.
- [23] J. R. Johler and L. C. Walters, "Propagation of a ground wave pulse around a finitely conducting spherical earth from a damped sinusoidal source current," IRE TRANS. ON ANTENNAS AND PROPAGATION, vol. AP-7, pp. 1-10; January, 1959.
- [24] W. Furry, "Tables of the Modified Hankel Functions of Order One-Third and of their Derivatives," Harvard University Press, Cambridge, Mass., 1945.
- [25] J. R. Johler and C. M. Lilley, "Ground conductivity determinations at low radiofrequencies by an analysis of the spheric signatures of thunderstorms," *J. Geophys. Res.*, vol. 66, pp. 3233-3244; October, 1961.
- [26] J. R. Wait, "Terrestrial propagation of VLF radio waves," *J. Res. NBS*, vol. 64D, pp. 153-204; March-April, 1960.
- [27] J. R. Johler and J. D. Harper, Jr., "Reflection and transmission of radio waves at a continuously stratified plasma with arbitrary magnetic induction," *J. Res. NBS*, vol. 66D, pp. 81-99; January-February, 1962.
- [28] A. G. Booker, "Some general properties of the formulas of the magnetic-ionic theory," *Proc. Roy. Soc. (London), A*, vol. 147, p. 352; November, 1934.
- [29] L. M. Brekhovskikh, "Waves in Layered Media," Academic Press, Inc., New York, N. Y.; 1960.
- [30] C. O. Hines, "Wave packets, the Poynting vector and energy flow, pts. I-IV," *J. Geophys. Res.*, vol. 56, pp. 63-72, March; pp. 197-220, June; pp. 535-544, December, 1951.
- [31] A. J. Ferraro and J. J. Gibbons, "Polarization computations by means of multislab approximation," *J. Atmospheric and Terrest. Phys.*, vol. 16, pp. 136-144; October, 1959.
- [32] A. H. Waynick, "The present state of knowledge concerning the lower ionosphere," *Proc. IRE*, vol. 45, pp. 741-749; June, 1957.
- [33] J. C. Seddon and J. E. Jackson, "Rocket Arctic Ionospheric Measurements," Internatl. Geophys. Soc., IGY Rocket Rept. Ser., No. 1, pp. 140-148; 1958.
- [34] M. Nicolet, "Aeronomic Conditions in the Mesosphere and Lower Ionosphere," Pennsylvania State Univ., University Park, Sci. Rept. No. 102; 1958.
- [35] J. R. Johler and J. D. Harper, Jr., "On the Effect of a Solar Disturbance on the LF Ionosphere Reflection Process," presented at 6th AGARD Ionospheric Res. Committee Meeting, Naples, Italy; May 15-18, 1961. "On Effects of Disturbances of Solar Origin on Communications" (to be published, AGARD-GRAPH, Pergamon Press).
- [36] A. V. Phelps, "Propagation constants for electromagnetic waves in weakly ionized, dry air," *J. Appl. Phys.* vol. 21, pp. 1723-1729; October, 1960.
- [37] P. Molmud, "Langevin equation and the ac conductivity of non-Maxwellian plasmas," *J. Phys. Res.*, vol. 114, pp. 29-32; April, 1959.
- [38] R. Jancel and T. Kahan, "Theorie du Complage des Ondes Electromagnetiques Ordinaire et Extraordinaire dans un Plasma Inhomogene et Anisotrope et Conditions de Reflection," *J. Phys. et Radian*, vol. 15, pp. 136-145; 1955.
- [39] J. R. Wait, private communication, November, 1960.

ADDITIONAL REFERENCES

- K. G. Budden, "Radio Waves in the Ionosphere," Cambridge University Press, London, England; 1961.
- J. A. Ratcliffe, "Physics of the Upper Atmosphere," Academic Press, London, England; 1960.
- J. A. Ratcliffe, "Magneto-Ionic Theory and its Applications to the Ionosphere," Cambridge University Press, London, England; 1959.

A SHORT BIBLIOGRAPHY ON GROUND WAVE PULSES

- L. Brillouin, "Über die Fortpflanzung des Lichtes in Dispergierenden Medien," *Ann. Phys.*, vol. 44, pp. 203-240; 1914.
- J. R. Johler, "Propagation of the Radiofrequency Ground Wave Transient over a Finitely Conducting Plane Earth," *Geofis. pura e appl.*, vol. 37, p. 116; February, 1957.
- J. R. Johler, "Transient radiofrequency ground waves over the surface of a finitely conducting plane earth," *J. Res. NBS*, vol. 60, p. 281, April, 1958.
- J. R. Johler, "A Note on the Propagation of Certain LF Pulses Utilized in a Radio Navigation System," U. S. Dept. of Commerce, Office of Tech. Services, Washington, D. C., NBS Tech. Note No. 118 PB 161619; October, 1961.
- J. R. Johler and L. C. Walters, "Propagation of a ground wave pulse around a finitely conducting spherical earth from a damped sinusoidal source current," IRE TRANS. ON ANTENNAS AND PROPAGATION, vol. AP-7, pp. 1-11; January, 1959.
- J. Keilson and R. V. Row, "Transfer of transient electromagnetic waves into a lossy medium," *J. Appl. Phys.*, vol. 30, p. 1595; October, 1959.
- B. R. Levy and J. B. Keller, "Propagation of electromagnetic pulses around the earth," IRE TRANS. ON ANTENNAS AND PROPAGATION, vol. AP-6, p. 56-65; January, 1958.
- V. V. Novikov, "Propagation of a radio pulse over the surface of a plane homogeneous earth," *Vestnik Leningrad. Univ., Ser. Fiz. i Khim.*, Nrlo (Issue 2), p. 16; 1960.
- V. V. Novikov and G. I. Makarov, "The propagation of pulse signals over a plane homogeneous earth," *Radiotech. Electron.*, vol. 5, p. 708; April, 1961.
- C. L. Pekeris and Z. Altermann, "Radiation from an impulsive current in a vertical antenna placed on a dielectric ground," *J. Appl. Phys.*, vol. 28, p. 1317; November, 1957.
- A. Sommerfeld, "Über die Fortpflanzung des Lichtes in Dispergierenden Medien," *Ann. Phys.*, vol. 44, pp. 177-302; October, 1914.
- B. van der Pol, "On discontinuous electromagnetic waves and the occurrence of a surface wave," IRE TRANS. ON ANTENNAS AND PROPAGATION, vol. AP-4, pp. 288-293; July, 1956.
- J. R. Wait, "A note on the propagation of the transient ground wave," *Canad. J. Phys.*, vol. 35, p. 1146; September, 1957.
- J. R. Wait, "Propagation of a pulse across a coastline," *Proc. IRE (Correspondence)*, vol. 45, pp. 1550-1551; November, 1957.
- J. R. Wait, "The transient behaviour of the electromagnetic ground wave over a spherical earth," IRE TRANS. ON ANTENNAS AND PROPAGATION, vol. AP-5, pp. 198-205; April, 1957.
- J. R. Wait, "Transient fields of a vertical dipole over homogeneous curved ground," *Canad. J. Phys.*, vol. 34, p. 116; January, 1956.
- J. R. Wait, "On the waveform of a radio atmospheric at short ranges," *Proc. IRE (Correspondence)*, vol. 44, p. 1052; August, 1956.